AUTOMATIC TEMPERATURE CONTROL SYSTEM FOR SEMICONDUCTOR DEVICES DURING RADIATION TESTING

A Thesis

by

TYLER ALAN LEW

Submitted to the Office of Graduate and Professional Studies of
Texas A&M University
in partial fulfillment of the requirements for the degree of

MASTERS OF SCIENCE

Chair of Committee,	Rainer Fink
Committee Members,	Byul Hur
	Jose Silva-Martinez
	Wei Zhan
Head of Department,	Reza Langari

May 2020

Major Subject: Engineering Technology

ABSTRACT

The proposed project focuses on the issue of inaccurate temperature control in a critical environment. Currently, there are two options with respect to radiation testing, in house radiation testing, or traveling to third party locations. In house radiation testing gives the ability to build temperature control environments around the beam. However, traveling to third party locations requires setups that must be portable and flexible in order to be used from place to place. A current temperature control system in use does not have the capability to achieve precise temperatures, as well as the need for manual implementation of the system to adjust the voltage line of the radiator. The current system operates with open loop control, meaning there is no automated feedback for adjustments. For an optimal control system in the radiation environment a Proportional-Integral-Derivative (PID) Omega Controller will be calibrated to achieve setpoint fluctuations of no more than ± 1 ℃. The Omega Controller's temperature control will then be compared to the current open loop control system for to determine the difference of temperature control. After comparing the data between the two setups, a thermal camera will be implemented as part of the Omega control system. A thermal camera will use infrared imaging technology to conduct temperature measurements to a similar accuracy of the currently used type K thermocouple wire. The thermal camera measurements will act as a non-contact test method to measure true chip temperatures rather than output air temperatures. The data acquisition, comparison, and proposed end system will be presented in the following thesis.

ACKNOWLEDGEMENTS

I would like to thank my committee chair, Dr. Fink, and my committee members, Dr. Hur, Dr. Silva-Martinez, and Dr. Zhan, as well as Tom Munns for their support throughout the course of this research.

Thanks also go to my friends, the department faculty, and staff for making my time at Texas A&M University a great experience.

I would also like to thank Texas Instruments, specifically Joel Cruz-Colon, for their support throughout my research and the help given along the way.

Finally, I would like to thank my family, Gena Lopez, Keith Lew, Guillermo Lopez, and Savanah Boydston for their love and support throughout the process.

CONTRIBUTORS AND FUNDING SOURCES

Contributors

This work was supervised by a thesis committee consisting of Dr. Rainer Fink, Dr. Byul Hur and Dr. Wei Zhan of the Department of Engineering Technology and Industrial Distribution as well as Dr. Jose Silva-Martinez of the Department of Electrical Engineering.

All other work conducted for the thesis was completed by me, Tyler Lew, independently.

Funding Sources

This work was funded primarily by Texas Instruments through Texas A&M University.

NOMENCLATURE

TI	Texas Instruments
PID	Proportional-Integral-Derivative
DUT	Device Under Test
PCB	Printed Circuit Board
GCR	Galactic Cosmic Rays
LEO	Lower Earth Orbit
MEO	Middle Earth Orbit
HEO	Higher Earth Orbit
GEO	Geostationary orbit
GSO	Geosynchronous orbit
LET	Linear Energy Transfer
MEV	Mega Electron Volt
SEE	Single Event Effect
SEU	Single Event Upset
SET	Single Event Transient
SEFI	Single Event Functional Interrupt
DRAM	Dynamic Random-Access Memory
SRAM	Static Random-Access Memory
SEL	Single Event Latch-Up
SEB	Single Event Burnout
ALT	Accelerated Life Tests
MOSFET	Metal Oxide Semiconductor Field Effect Transistor
RTD	Resistance Temperature Detectors
TFU	Thermal Force Unit

TABLE OF CONTENTS

Page

LIST OF FIGURES

LIST OF TABLES

1. INTRODUCTION

1.1 Problem

Most companies conducting thermal and life cycle tests use temperature control chambers, in which the devices are sealed and introduced to an array of temperatures ranging from a specified minimum temperature to a specified maximum temperature. In thermal testing, generally there is no need for any other aspects to be tested, other than the device's ability to turn on or off or generate a signal. Because the only equipment necessary is a power source and a measurement instrument, climatic chambers can be built with, or around these devices. In contrast, when looking at thermal or life cycle testing during radiation testing, there are many other aspects that are involved. The most glaring issue with conducting these tests during radiation testing is the need for the device under test (DUT) to be lined up in a clear path for the radiation beam to radiate it. Alter technologies currently have a set up for low temperature testing that involves using a climatic chamber for temperature control and a vacuum chamber for the vacuum of space simulation [1]. A vacuum setup would use liquid nitrogen to be deposited into the climatic chamber to cool the DUT down, or hot air to be pumped in to heat the DUT up. Their design measures the temperature of the climatic chamber with thermocouple wiring in close to direct contact with the DUT which is fed back to a PID controller [1]. In house setups are only viable for a company which conducts radiation tests in their own labs.

There is a need to create an accurate temperature control setup that will be viable for those needing to travel to conduct tests. Texas Instruments conducts their radiation testing at the Cyclotron Institute at Texas A&M University, which requires the control system to be designed around the setup of the radiation beam., TI uses a standalone transformer as a heating element connected to a pressurized air system to expel hot air and heat the DUT via the ambient air

temperature. Although the system has worked as a temporary fix to the issue, however there are two issues with the current setup. First, the temperature reading is dependent on the placement of a thermocouple wire which is taped onto the printed circuit board (PCB) as close to the DUT as possible. Even though the wire is very close, generally within 2 cm, to the DUT it cannot touch the DUT due to the radiation beam needing a clear path to the DUT. The temperature reading obtained is not a perfect representation of the true temperature of the DUT. The second issue is the control of the setup which is open loop. There is no way to automatically adjust the temperature of the air without manual interruption. With no feedback loop, the output temperature will never sit at the desired temperature. Because TI is already testing at level 2 military standards, 125 ℃, they do not want to exceed 125 ℃, however with the open loop, exact accuracy is not achievable. Lack of closed loop control creates certain issues such as overshoot with respect to the desired temperature, as well as settling time issues to the true temperature. The output air of open loop control can cause issues in DUT temperature due to a constant output air temperature that could cause the DUT temperature to continually rise. A continuous rise in DUT temperature would cause thermal testing to be conducted at higher than the desired 125 ℃. Continuous rises in temperature would cause issues with settling time as well. With beam time on a strict schedule, the less time spent waiting to settle, the more tests can be done, making better use of testing time. Having a way to decrease overshoot, ensure the DUT temperature will remain constant, and achieve the desired temperature as quick as possible would drastically improve the test setup for temperature control during radiation testing.

1.2 Proposal

A portable closed loop control system must be implemented in order to achieve accurate temperature control, while still being easily transportable from location to location. As a solution, a PID controller from Omega Engineering, a leading company in temperature control equipment, was procured. The controller from Omega is small enough to be easily packaged up and transported from location to location, as well as small enough to be implemented with the overall test setup without interfering with things such as other measurement probes and the radiation beam itself. The Omega Controller can utilize many types of input sensors, including 10 thermocouple types, as well as DC voltage or DC current, providing the control system with temperature readings in a similar method to the open loop system via thermocouple wire, as well as the ability for feedback through a thermal camera [2]. By adjusting the location of the thermocouple wiring to direct contact with the air output location, we can achieve more accurate temperature readings for the output air. Because the controller is a closed loop system, the true output will be centered around the setpoint, adjusting as it goes above and below the setpoint, rather than the open loop system which looks to only rise to a desired setpoint with no feedback. Feedback will ensure the air contacting the DUT is truly the desired temperature and will heat up to the specified temperature for accurate stress and life cycle testing to be completed. To achieve even more accurate temperature feedback and control, a thermal camera will be implemented as part of the system. By using a thermal camera which can transmit the temperature data as images, temperature feedback of the DUT is achieved rather than temperature of the air. If the DUT temperature can be fed back, there can be even more accurate temperature control as well as even more certainty that the DUT is being tested at the desired temperature. A combination of these feedback options gives previously unachievable temperature control accuracy.

2. BACKGROUND

2.1 Radiation Testing

Texas Instruments consists of many departments ranging from their most well-known products such as calculators to the production and testing of many microcontroller chips such as the ones powering your phones, laptops, and many other electronics used every day. One of their lesser known departments is the Space Power department which is responsible for testing chips and components which will be commissioned and sent into and operate in space, most notably in the lower orbit atmosphere on satellites. Because these chips will be operating in space, they will experience different operating circumstances than they would encounter on Earth. One of the most notable differences is the amount, and type, of radiation that will bombard the part during its life cycle.

There are many different radioactive particles that the part may encounter including Galactic Cosmic Rays (GCRs), solar radiation, and radiation belts [3]. To determine the amount of radiation to mimic, the amount of magnetic shielding from the Earth must be determined. The five orbits are categorized as Lower Earth orbit (LEO), Medium Earth orbit (MEO), geostationary orbit (GEO), geosynchronous orbit (GSO), and High Earth orbit (HEO). The orbits are visualized in Figure 1[4].

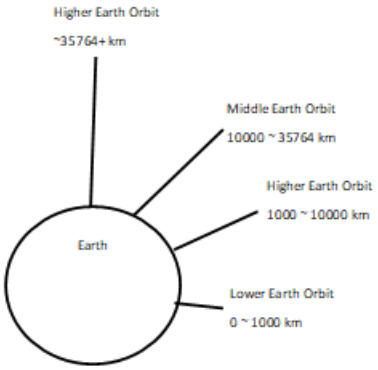

Figure 1. Earth Orbits

LEO is generally used for satellites which require minimal communication delays with short orbital periods, whereas MEO is generally used for GPS, communication, and science observation missions. [3] GSO and GEO mimic the Earth's rotation and vary between whether they hover above the equator, GSO, or over the North and South poles, GEO [3]. Above GSO and GEO is HEO, which is generally used for missions such as deep space monitoring due to the need to be beyond electromagnetic traffic in lower orbits [3]. Because the tests are generally done in order to mimic the LEO, the goal is to create the linear energy transfer (LET) the device will encounter in its orbit, normally referred to in terms of electron volts scaled to 10^6 per nucleon (MeV/n) [5]. LET measurements help to characterize components by determining the displacement damage dose (DDD) as well as the rate of single-event effects (SEEs) that will be accumulated [3]. Although the "L" in LET stands for linear, LETs are nonlinear, the linear portion of the term refers to the fact it is a function of energy loss per unit length [3]. Determining the LET and range, or the amount of target material needed to reduce an ions kinetic energy to 0, can be used to determine the Bragg peak, or the peak in the LET curve [3]. Bragg peaks help in understanding the amount of interactions the ion has with the matter it is traveling through, as well as the amount of shielding necessary for the material under test to help protect it [3]. In order to achieve high amounts of radiation, Texas Instruments will work with the Cyclotron Institute at

Texas A&M University, where beam lines are used to simulate the effects of ionizing radiation on electronic systems [6]. The cyclotron uses a beam degrader system to provide mimicked LET into electronic devices with beams of 15, 25, or 40 Mega Electron Volt per micron (MeV/u). The specific heavy ion beams the Cyclotron Institute offers which TI uses are Argon (Ar), Copper (Cu), Krypton (Kr), Silver (Ag), Xenon (Xe), and Presidium (Pr) [6].

There are three main methods used to help reduce the amount of exposure, limiting the time near radiation, maximizing the distance between the device and the radiation, and shielding against the radiation [3]. Because the devices will be operating in space, there is no way to truly control the time or distance in/from radiation, therefore, how well devices can hold up to radiation can only be improved upon by including radiation shielding [3]. Using metal barriers, ceramic plates, or even full enclosures provides necessary shielding [3]. Shielding can help to minimize the incident flux of radiation, which will help to reduce the dose of radiation received, as well as the total number of SEEs [3]. If the dose and the number of SEEs can be limited, then devices which operate in the high radiation environments can last longer and operate truer to their non-radiated specifications. Therefore, it is important to investigate the different types of SEEs and how each one can impact the DUT. If these, and the number of allowable events of each type, are known, then it is possible to determine how well the DUT will perform and whether it can be approved for space.

When electronic devices receive any amount of radiation, they begin to experience SEEs which can cause permanent damage to the device in some cases [7]. There are multiple ways to categorize a SEE, such as destructive and non-destructive. Generally, non-destructive SEEs, fall into single-event transients (SETs), single-event upsets (SEUs), and single-event functional interrupts (SEFIs) [3]. SETs are events that will always happen when ions go through an electronic

device, the transient is the origin of the SEEs from which all other events are derived [3]. SEUs occur when radiation enters a node of digital storage, such as in dynamic random-access memory (DRAM) or static random-access memory (SRAM) [3]. These types of events can cause issues for data being obtained and processed. SEFIs tend to occur in digital devices when bits are flipped that are part of a systems control operations [3]. Each of the previously mentioned failures can cause issues, however they are non-destructive failures, meaning each failure will not cause permanent damage to the device and will either return to normal operation on its own or after a reset. Although single-event latch-ups (SELs) can be non-destructive, most are destructive, in which the devices are permanently damaged and the circuitry surrounding it are permanently damaged or destroyed [3]. SELs occur when maximum current limit is reached, the difference between a destructive and non-destructive SEL is whether permanent damage occurs from the excess current being sent through the circuitry [3]. SELs are not the only destructive SEEs, as there are also single-event gate ruptures (SEGRs) and single-event burnouts (SEBs) [3].

The ability to determine if a SEE can cause a device to break with the inability to return to operation on its own could prevent a much larger problem from occurring with the overall system. TI attempts to mimic the lower orbit atmospheres as closely as possible. Operating tests at the Cyclotron Institute at Texas A&M University, TI can dose devices and PCBs with heavy ion beams in order to perform the necessary SEE tests to determine the quality of parts. Some tests, such as the non-destructive tests do not need to be performed any higher than room temperature, however destructive tests like the SEL test must be conducted at maximum, or junction, temperature [3]. Because these extreme tests can be some of the most important tests in determining the devices ability to operate without being destroyed, a way to accurately control temperature is required.

2.2 Thermal Testing

In general, there are many needs for thermal testing in order to ensure devices, chips, and overall PCBs are viable. The two most important reasons, however, are to ensure the product can withstand a range of temperatures from its minimum operating temperature to its maximum and to simulate a lifecycle testing. When looking into thermal cycle testing, there are generally three accepted levels, the first being up to 0 ~ 85 ℃, the second being up to 0 ~ 125 ℃, and the third being up to 0 ~ 150 ℃ [8]. These levels, which were originally based off military standards that are now technically obsolete, are still considered to be the benchmark numbers for thermal testing, specifically used by NASA for the testing of their equipment [8]. Stress tests require the tests to be performed at the accelerated temperatures. Thermal shock, which is initiated by Heat steps can be used to evaluate mismatch issues in electronic systems as well as failures with functional tests and the actions necessary for corrective measures [9]. Initial thermal tests check for unidentifiable, but relatively easy fixes, to be determined. Although initial thermal tests are not as in depth or as important to the overall life of the device, the temperature at which the devices are tested is the most important aspect of the test. Therefore, a way to control temperature accurately is necessary.

Thermal control and thermal cycling can also be used for accelerated life tests (ALTs). These types of tests can check for failure mechanisms dependent on electro-thermal environments and check for the overall reliability and robustness of parts [10]. When looking at specific thermal tests for ALTs, thermal cycling can be used to determine solder joint cracking and delamination, whereas high temperature testing can be used to determine failure modes for MOSFETs and other

power handling or control components [10]. Performing both temperature cycling and high temperature tests can be used to define long term reliability of components specific to the environment they will be operating in [10]. The ability to accurately characterize the life of a device holds value in situations where components or devices as a whole are not easily interchangeable.

A third type of thermal testing is using infrared camera technology in order to create thermal images of objects and DUTs in order to determine temperature without the need for thermocouple wires. Thermal imaging provides quick feedback either on the camera itself, or to a nearby device connected to the same network for data transmission and data processing. With respect to thermal imaging, these cameras create a way to visualize the infrared spectrum by converting infrared wavelengths to a visual spectrum for humans [11]. The main difference in thermal feedback for thermal cameras compared to thermocouple wires/probes or RTDs, is thermal cameras offer a non-contact test method [11]. With a non-contact test method testing can be done in inaccessible or hazardous areas, meaning thermal testing can be useful for radiation testing [11]. More accurate representation of testing can be achieved through measuring the DUT temperature, not just temperature measurements with proximity to the DUT. Along with the ability to test without having to contact the device, the feedback for measurements can be in the form of images, something not possible with thermocouples or RTDs [11]. Having images to refer to can help to give more overall feedback than a simple numerical reading, dataset, or graphical representation.

Two more prominent types of thermal measurement tools are thermocouple wires/probes and RTDs, which are contact methods. Each of these contact measurement methods has pros and cons, with each excelling at different types of thermal measuring. The basic setup of thermocouple measurements is the implementation of a circuit composed of two different metals to generate

EMF at the junctions at the ends of the two metals, if the metals are at different temperatures [12]. Temperature measurements are made with instruments using cold-junction temperature and the Seeback voltage, defined by the National Institute of Standards and Technology, account for the nonlinearity of these measurements [12]. Thermocouples provide extremity temperature measurements with a low limit of roughly -270 ℃ up to 1800 ℃ or higher [13]. The accuracy of the thermocouple is dependent on the consistency of the cold junction temperature [13]. RTDs or thermal resistance on the other hand are generally used for lower temperature measurements, generally only up to about 500 ℃ [13]. RTDs use the character of the conductor resistance, which changes with temperature, where the accuracy of the measurement is based on the stability of the physical and chemical properties of the material [13]. The most common types of RTDs are Platinum and copper [13]. Although RTDs have a more linear correlation between temperature and resistance, with the NIST table, thermocouples have a very easy way to convert raw readings to accurate temperature readings. Thermocouples also have a quicker response time from measurement to reading compared to RTDs, therefore, having thermocouples as part of a PID control system can positively affect the rise time and settling time to the setpoint.

To obtain true temperature control, most thermal testing is done in climatic chambers. Climatic chambers are enclosures that provide climate conditions without the influence of the environment outside the climatic chamber [14]. In general, these chambers are larger enclosures, required to be placed in a specific laboratory, sometimes climate controlled itself. Utilizing control algorithms within these climatic chambers thanks to quick feedback from thermocouple wires or RTD sensors, can achieve better accuracy and better stability of the systems [14]. The most popular method for control is through the combination of PID controllers, heaters, and temperature sensors [14]. Through closed loop control the chamber measures the output temperature and the

temperature of its interior, which is fed back into the control loop to adjust the input temperature. [14]. Climatic chambers offer vacuum sealing, but by taking elements of the overall system it is possible to implement similar control and accuracy in a portable package.

2.3 PID Controllers

A PID controller or proportional, integral, derivative is a type of control system which helps processes errors to regulate desired outputs. Most notably, PID controllers are used for energy production, transportation, manufacturing, and many other automated systems [15]. PID controllers can be combined with logic, functions, and other system blocks for predictive control [15]. With the original idea of the PID controller being created in 1911 by Elmer Sperry, the first true PID controller was designed in 1939 by the Taylor Instrument Companies [16]. By revolutionizing the Fulscope pneumatic controller by combining it with their Stabilog pneumatic controller, TIC created a controller with pre-act capabilities, which achieved proportional and reset control actions, Hyper-reset, which accounted for the derivative of the error signal, and floating, which accounted for the integral of the error signal [16]. In 1942, the Ziegler and Nichols tuning rules helped engineers to set appropriate parameters of PID controllers on open-loop tests first and then closed-loop tests [16].

CL RESPONSE	RISE TIME	OVERSHOOT	SETTLING TIME	S-S ERROR
Kp ↑	Decrease	Increase	Small Change	Decrease
Ki ↑	Decrease	Increase	Increase	Eliminate
Kd ↑	Small Change	Decrease	Decrease	Small Change

Table 1. Closed Loop Responses of PID Controller

When breaking down the PID controller, it is important to discuss each aspect of the PID controller. For an overview, referring to the Table 1, it is important to understand what proportional, (Kp), integral, (Ki), and derivative, (Kd), control do in a closed loop system. Kp will look to decrease rise time and steady state error, however too high of a Kp value can lead to an increase in overshoot [17]. Ki will look to decrease rise time, with an overall goal of eliminating steady state error. Too high of a Ki value can lead to an increase in overshoot as well as an increase in settling time [17]. Kd will look to decrease overshoot and decrease the settling time [17]. A combination of each of the three aspects of the system will have a system that will rise to the setpoint quickly, have small overshoot, and settle to the setpoint quickly with little to no steady state error, or oscillation above or below the setpoint.

In order to discuss what each component of the PID controller does, an in-depth look is required. There is always steady state error in proportional control, therefore with increasing gain, there will be decreasing error [15]. The Proportional control adjusts the output in proportion to the error, therefore if the error increases, so does the control, proportionally speaking [18]. The proportional setting is known as the controller gain, the higher the gain, the higher amount of proportional control. However, if the gain is too high, the control loop can oscillate and become unstable, if too low, the loop may not respond to error or set point changes [18]. The integral control provides the automatic reset, which increments or decrements the controller's output in order to reduce error, with the end goal of driving the output error to zero [18]. The integrals time setting helps to determine the speed at which the integral control adjusts the output error, a longer time creates a slower controller, however too short of a time will create an oscillating loop which will become unstable [18]. Derivative control is based on the rate of change of the error and is based on its time setting. The longer the time setting, the more action is produced, however too

large of a time setting will lead to oscillations and cause the control loop to become unstable [18]. With respect to temperature control, the derivative portion of the PID controller holds its importance in the loop responding faster than just a PI controller [18].

As PID controllers have become more widespread and are still the leading closed loop feedback system, the innovations in software surrounding the controllers have become more complex and more efficient controllers to be created. Software such as LabVIEW has created the ability to control PID controller instruments or instruments part of a PID control system to become more autonomous. LabVIEW uses Virtual Instruments (Vis) to construct diagrams consisting of programming blocks and customizable front panels that create a graphical user interface (GUI). Feasibility of use of the GUI provides even those without much knowledge of PID controllers or the overall control system the ability to adjust and control as needed. If the transfer function is known, the user should be able to adjust the values of Kp, to improve rise time, Ki, to eliminate steady state error, and Kd, to improve overshoot, in order to make the PID controller operate optimally [17].

PID controllers can be implemented as part of many different types of systems. In the world of temperature control, many of the best systems utilize the ability of PID controllers to adjust inputs based on outputs to constantly adjust temperature dependent environments. By tuning the controller gain, integral, and derivative time, PID controllers can be used to adjust heating and cooling of climatic chambers and other temperature control systems [14]. In systems with only a heater control, PID controllers will generally control the power to the heating element, in the case of not a high enough temperature, power will be delivered to the heater, however when temperature is above the setpoint, power will no longer be delivered [14]. The main dependency on the ability of a PID controller to achieve high control and accurate adjustments is based on the ability of the

PID to accurately calculate the error [14]. The better the type of sensors measuring either the output of the heater or the environment of the climatic chamber or temperature control system, the better the PID controller will work. Pairing with accurately tuning the P, I, and D values of the controller will provide for optimal accuracy, quick response time, and desired temperature control. Although climatic chambers offer the best environment for PID controllers to operate with respect to temperature control, having the ability for a small PID controller to operate in an environment with a GUI could achieve similar accuracy of the climatic chamber, while still not interfering or getting in the way of other components of the system.

3. SYSTEM ARCHITECTURE

3.1 Open Loop Control System – Detailed Setup

The current open loop temperature control setup used during cyclotron testing consists of a standalone transformer, an air pressure system, and a metallic heating output tube for the hot air. The transformer must be plugged into a wall outlet, either 120 V or 240 V, and will adjust the output voltage dependent on physical manipulation of the dial on the transformer. The transformer dial reads from 0 V to 140 V, however if plugged into a 120 V outlet, the transformer cannot exceed the line voltage of 120 V. Connected to the transformer is the metallic heating output tube. The tube is connected via 3-prong plug, which plugs directly into the transformer. The heating element takes the output voltage of the transformer and heats up to the desired temperature. For the tube to function properly, it is connected to a pressurized air system which ensures 20 ~ 60 psi of air flow is present. Air flow is displayed by an air pressure gauge which connects the tube to the overall air pressure system. In the case of the specific setup, there is an extra air pressure tube which can connect between the air pressure gauge and an air pressure outlet.

Because the current system is under open loop control, there is no feedback of the output temperature to the transformer. In general testing purposes, there is a piece of thermocouple wire or RTD which is hooked up to data acquisition device which feeds back a temperature reading which is converted to ℃ in LabVIEW or by a data acquisition devie and then shown in real time on a device or GUI created in LabVIEW. During the current analysis, the PXI test system was replaced with a digital temperature probe which gives real time feedback based on the ambient air temperature it reads. In order to ensure accuracy and to mimic the distance to a DUT, the probe was placed at .5 inches or 1.27 centimeters away from the output tube. Because there is also no

GUI present, data was acquired through the visual reading of the digital temperature probe and input into Excel.

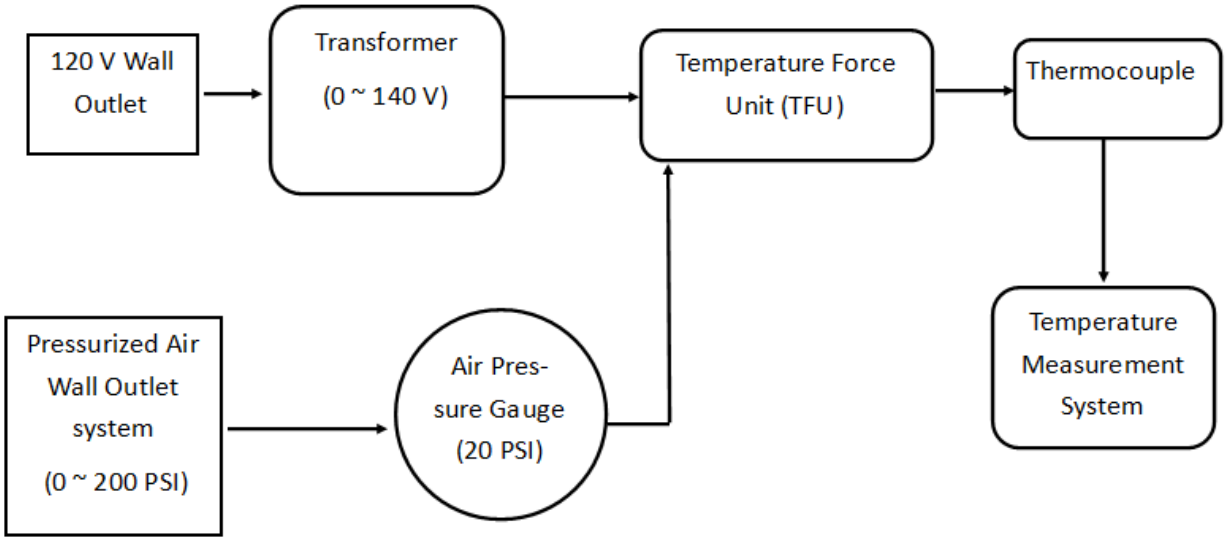

Figure 2. Open Loop Control System Block Diagram

The block diagram in Figure 2 gives a visual representation of the open loop control offered by the current setup. The temperature is dependent on two aspects, the voltage output of the transformer, which is related to the angle of the dial of the transformer, and the heater, which accepts the voltage output and heats proportionally. As stated, the heater will take in the voltage and adjust the air exiting the heater to the desired temperature, in Celsius, through the equation shown in the figure. Since the transformer is open loop control, the output temperature is not fed back into the input, therefore it will be regulated by the dial position, it cannot be adjusted without outside forces. Along with manual adjustment, the lack of feedback causes the output temperature to continually oscillate above and below, generally continuing to rise, from the desired temperature. Lack of elimination of steady state error causes the system to lack the accuracy necessary for temperature control compared to climatic chambers.

Figure 3. Standalone Transformer

The standalone transformer in Figure 3 is the Powerstat 3PN116C Variable Transformer. The transformer is rated for 120 AC Voltage (VAC) input voltage and up to 140 volts (V) output voltage with a max of 10 ampere (A) output current [19]. The variable transformer is required to adjust and regulate the input voltage for temperature control at the output. The transformer is manually controlled by rotating the dial between 0 and 140 both clockwise and counterclockwise. The radiator receives the input voltage from a 3-prong electrical plug and outputs from a 3-prong electrical outlet.

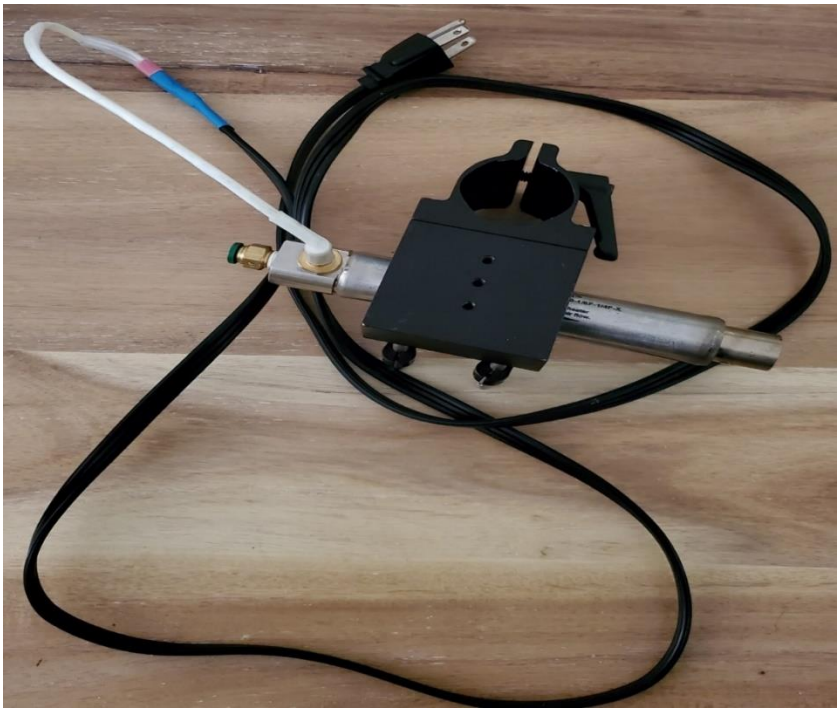

Figure 4. Farnam Cool Touch 050 Heater

The heater in Figure 4 connects to the Powerstat 3PN116C variable transformer by connecting its 3-prong electrical plug into the variable transformer's 3-prong outlet. Pressurized air enters the metal tube from the left-hand side, where a pressure gauge is attached to ensure the air entering the tube remains at a constant pressure. The tube was placed as close to the DUT as possible to ensure the DUT will be heated, as well as to ensure the heating of other components will be minimized.

Figure 5. Pressurized Tube

The pressurized tube in Figure 5 acts as an attachment to an air pressure system so that the air pressure gauge is connected between it and the output tube in Figure 2. The tube receives up to 250 pounds per square inch (PSI) of pressure and has a locking design to ensure a sealed connection between itself and other attachments.

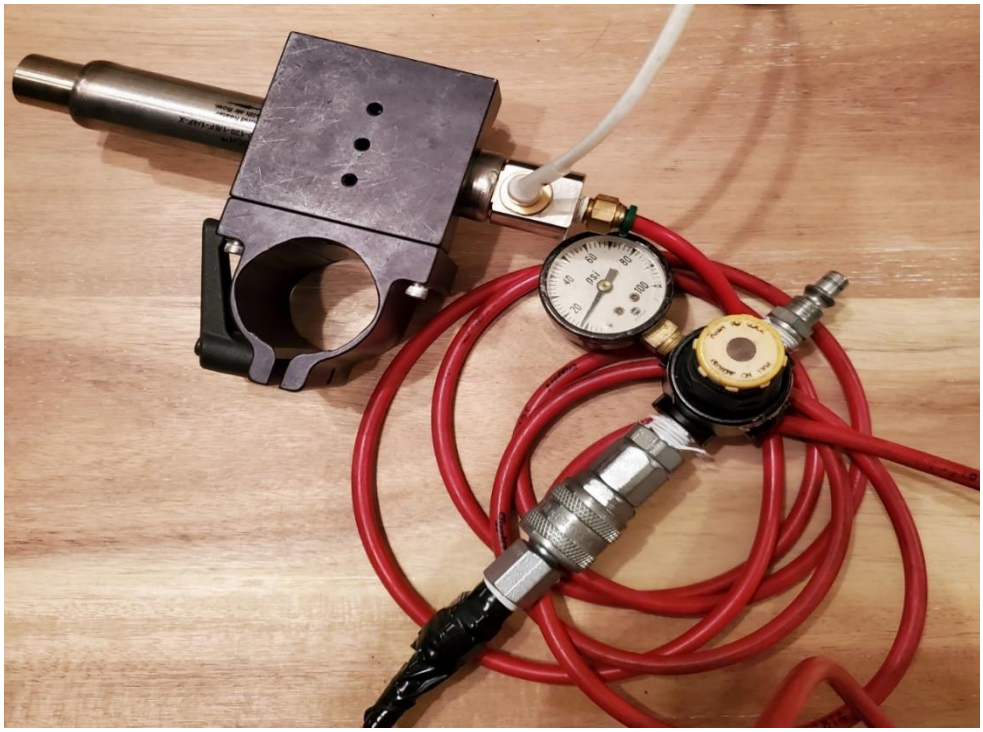

Figure 6. Air Pressure Gauge

The air pressure gauge in Figure 6 ensures the air flow going through the pressurized tubing remains at a constant PSI level to not harm the metallic output tube. The red tube attached to the pressure gauge attaches to the metallic tube to read the air flowing through the tube. If the air pressure remains at a constant PSI level, then the air flow will continue.

Figure 7. Overall System

The overall system in Figure 7 gives a visual of the connections necessary to complete the temperature control setup. The gray pressurized tube was connected to an outlet hose from the wall, which was connected to the air pressure gauge, which connected to the back of the metal heating tube. The metal heating tube was plugged into the transformer, which was then plugged into a 120 V outlet. Each aspect of the system provided the necessities in order to heat and output the air.

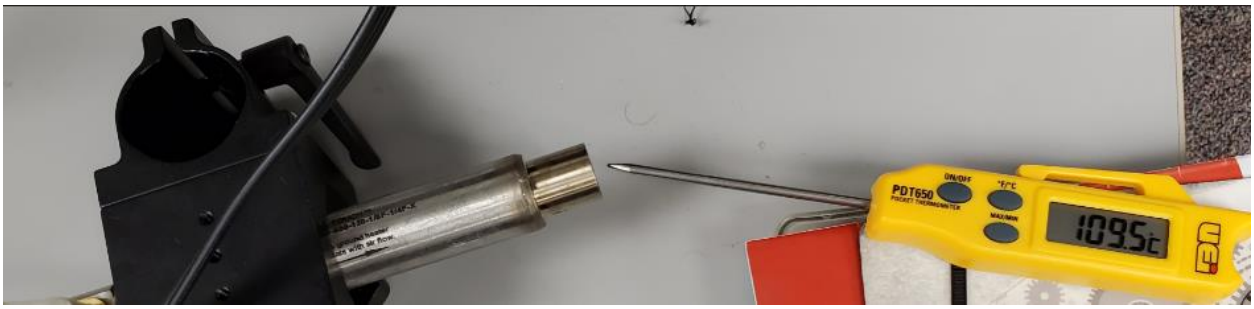

Figure 8. Open Loop Test Setup

The test setup in Figure 8 shows the temperature probe half an inch away from the edge of the metallic output tube. The probe is level with the middle of the output tube and is set to measure in degrees Celsius. The setup was used for all testing done with the standalone transformer, including determining the output based on dial readings, as well as the temperature versus time plots for the system.

3.2 Omega Controller – Detailed Setup

The Omega controller temperature control system will consist of the controller, the heating element and output tube, a pressurized air system, and a GUI. The Omega controller was directly connected to a laptop in order to run a GUI powered by LabVIEW, which took input from the computer transmitted over serial connection. The GUI also took the temperature readings from the Omega controller which gave graphical representation of temperature versus time. The heating element, which was plugged into the output terminal of the Omega controller will took the setpoint configuration and then used the power from the controller to heat to the desired temperature. In initial testing, the only feedback into the controller and the GUI will be from a thermocouple wire, which was connected directly to the output edge of the heating tube. The TFU reading was fed back into the controller as part of the closed PID loop. In order to operate the heating element safely, a pressurized air system was connected to the tube, like the setup for the standalone transformer.

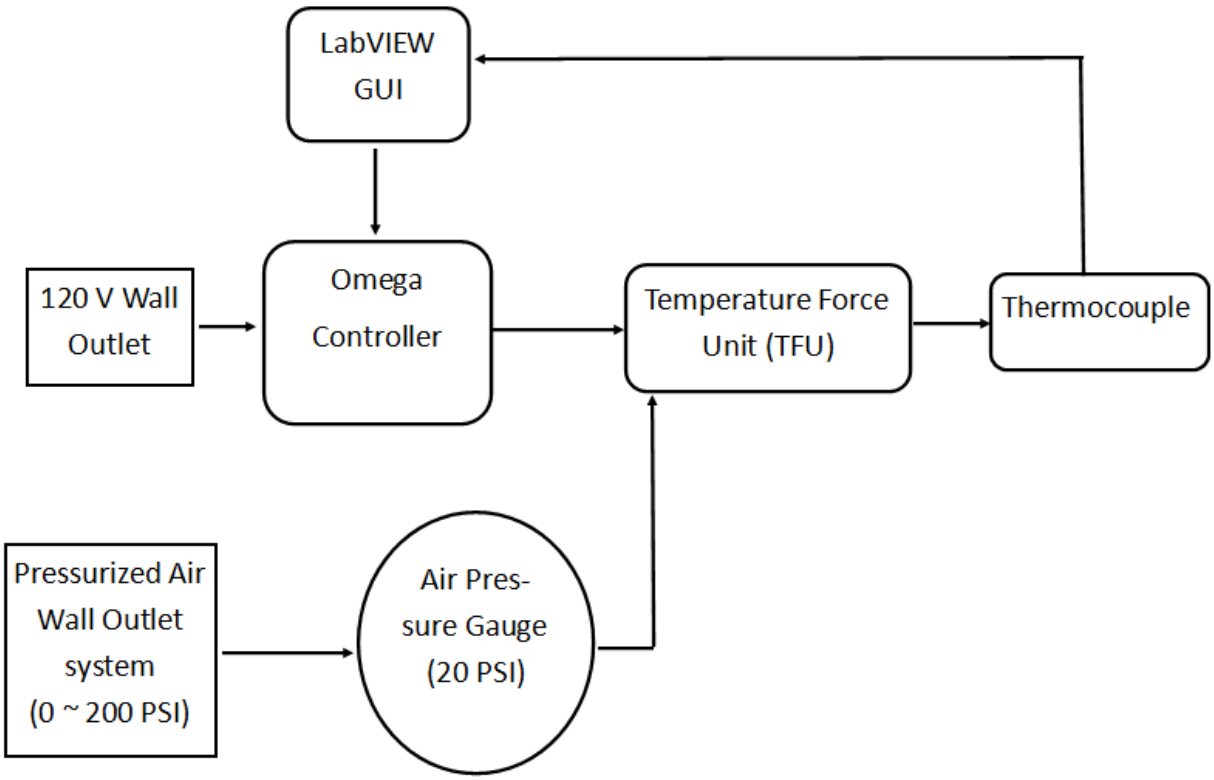

Figure 9. Omega Controller Block Diagram

The temperature control system for the Omega controller operates using closed loop control, meaning the output temperature is fed back into the input terminal in order to determine the error and necessary adjustments for the PID controller to make. The block diagram in Figure 9 illustrates PID control. The setpoint temperature was set to the desired temperature which then fed into the PID controller, whose settings are configured in LabVIEW. Once the settings are configured, the necessary configuration for the heater was sent to the heating element, which then heated the air flowing through it. The air was output at a specific temperature which will vary from the setpoint temperature, the air temperature was fed back into the input, and the difference, or error, was then sent back into the PID controller to make adjustments in order to change the output

temperature closer to the setpoint temperature. The system will continue to loop ensuring the steady state output temperature remains within ± .1 ℃ of the setpoint temperature.

Figure 10. Omega CSi8D-C24 Controller

The instrument in Figure 10 is an Omega Engineering "i" series benchtop digital controller. The controller itself features a dual 5 A control input and operates from 90 to 240 Vac at 50/60 Hz [20]. The controller is connected to a heater which adjusts internally through readings from sensor(s). These sensors could be thermocouple probes, RTD, or voltage/current readings. In the testing process for the Omega Controller, both thermocouple wires/probes, as well as voltage/current measurements which were obtained through thermal camera feedback.

Figure 11. Back of Omega Controller

In Figure 11, the back of the omega controller shows possible input and output connections for the controller. The main connections used in testing were the AC MAINS INPUT, for the outlet voltage, the OUTPUT 1 for connection to the heater, and the wired INPUT's for thermocouple wiring. With these connections, the controller received all information via the inputs and ensured the adjustment of the heater output a controlled temperature.

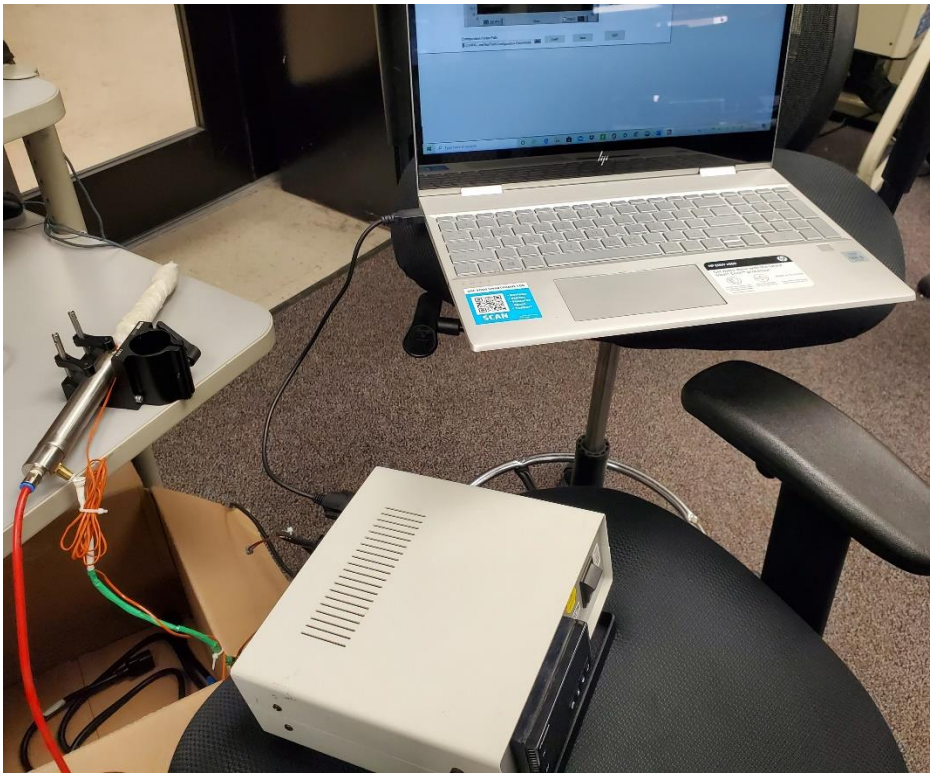

Figure 12. Omega Controller Test Setup

The setup in Figure 12, shows the heater (Metallic element) connected to the OUTPUT 1 slot, as well as the brown thermocouple wiring connected to the INPUT connections. With the AC MAIN INPUT connection connected to a wall outlet, the omega controller receives power from the outlet, would read the output temperature from the heater with the thermocouple wire, accept the read temperature as an input, and adjust the output temperature to reach the desired value. Further testing will use the thermal camera as well as the thermocouple wiring to ensure the correct measurement element is connected for fast and accurate temperature adjustment.

3.3 Thermal Camera

Figure 13. Huepar HTi80P Thermal Camera (Huepar, 2020) [21]

The Huepar HTi80P thermal camera, seen in Figure 13, is a small package, commercially available camera, with a temperature measurement range of -10 ℃ to 400 ℃ [21]. The accuracy of the measurements is ± 2.0 ℃ and has a measurement resolution to 0.1 ℃. The display with resolution of 320x240 pixels for clear images and video during testing. The thermal camera operates in a wavelength range of 8 um to 14 µm for a color palette feedback of rainbow, iron red, white heat, and fast thermal tracking, depending on the type of visual feedback the user desires. The battery is a 3.7 V, 1300 mAh rechargeable lithium battery, which receives a full charge in 2 to 2.5 hours. For storage purposes, the camera comes with a 16 GB SD card for multiple tests and images to be stored on the card and transferred over to a PC [21].

Figure 14. Camera Connectivity (Huepar, 2020) [21]

Figure 14 shows the ability to use the SD card to transfer images and feedback to PCs, the camera features direct connectivity through USB to PCs, providing quick and easy transfer without the need for extra components [21]. Easy transfer provides real time feedback on a PC and easy comparisons between other temperature test equipment.

4. MEASUREMENTS AND RESULTS

4.1 Open Loop Control System

The measurements are results in 4.1 will consist of both tables and graphical figures. Each table will precede its graph and will offer a numerical perspective on the data obtained. The graph which follows the dataset will give a visual representation of the data. Each dataset is based on temperature or error in temperature in ℃ versus either time (s) or dial setting in voltage. The first table is based on ideal operation of the standalone transformer in its open loop control system, the remaining tables and graphs are based on the real outputs of the system. The final table and final graph of the subsection offer a look into a comparison between the real operation of the open loop control system and the ideal operation of the open loop control system.

Ideal Temperature (℃) at Dial Reading (V)	
Dial Reading (V)	**Temperature (℃)**
45.0	**102.1**
47.0	**106.6**
50.0	**113.4**
51.0	**115.7**
53.0	**120.2**
55.0	**124.7**

Table 2. Ideal Open Loop Output Dataset

Table 2 shows the ideal temperature that is expected at the output based on the dial reading of the standalone transformer. An estimated ideal output shows a very linear output for the actual temperature in Celsius. With Table 2 in mind, the estimated dial voltages should be

within the range of 45 V to 55 V in order to achieve close to the desired output temperature of 125 ℃. The testing, then, for the real output will be conducted at the same dial voltages as described in the ideal table's dataset.

Time (s)	Temp ℃ at 45 V	Temp ℃ at 47 V	Temp ℃ at 50 V	Temp ℃ at 51 V	Temp ℃ at 53 V	Temp ℃ at 55 V
0	23.5	23.5	23.5	23.5	23.5	23.5
10	31	32.7	33	33.5	34.6	36
20	40.4	44.6	45.2	48.4	50.6	53.7
30	49.1	56.2	57.6	63.2	65.7	70.4
40	56.4	64.5	67	73.3	75.6	83
50	63.8	70.7	74.3	79.9	85.5	101.5
60	67.9	74.1	78.5	88.2	101.2	108.6
70	70.7	77.2	81.6	98.7	109.2	110.6
80	73.4	78.7	85.1	106.5	112.6	114.7
90	75.7	80.7	87	109.2	115.6	116.6
120	78.8	83.5	91.4	114.6	120.2	120.8
150	80.7	85.5	93.3	117.8	123.4	124.3
180	82.1	87.6	94.6	118.9	124.5	126.7
210	82.6	88.2	95.5	119.3	126.2	129
240	83.2	88.5	95.3	118.5	126.4	128.8
270	83.3	88.3	95.6	117.2	126.2	128.9
300	83.3	88.1	95.3	117.2	126.2	128.7

Table 3. Real Open Loop Output (℃) vs. Time (s) Dataset

The dataset in Table 3 gives the real temperature outputs based on the dial voltage readings on the standalone transformer. The dataset shows that after the 150 second mark, the transformer begins to reach steady state. By testing the temperature readings to for 150 seconds after achieving steady state, the averaged values are obtainable. Because the transformer's true output should be obtained only at the steady state point, the true outputs are the averaged-out temperature readings.

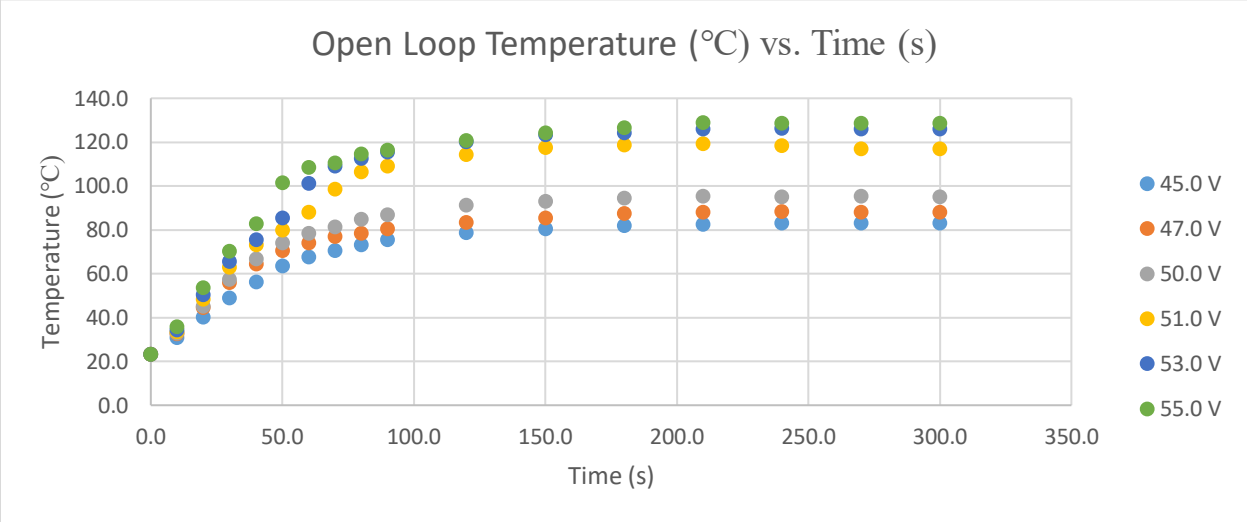

Figure 15. Open Loop Graphical Output

Figure 15 shows the graphical representation of the dataset from Table 3. As described in the dataset, the output temperature reaches steady state after approximately 150 seconds and remains very close to the highest temperature achieved at the dial setting with little overshoot and little undershoot.

Time (s)	Temp ℃ at 45 V	Temp ℃ at 47 V	Temp ℃ at 50 V	Temp ℃ at 51 V	Temp ℃ at 53 V	Temp ℃ at 55 V
150	80.7	85.5	93.3	117.8	123.4	124.3
180	82.1	87.6	94.6	118.9	124.5	126.7
210	82.6	88.2	95.5	119.3	126.2	129
240	83.2	88.5	95.3	118.5	126.4	128.8
270	83.3	88.3	95.6	117.2	126.2	128.9
300	83.3	88.1	95.3	117.2	126.2	128.7

Table 4. Real Open Loop Output at Steady State

Taking a closer look at what the true outputs are for the respective dial readings, the dataset in Table 4 is the temperature readings after achieving steady state. Because these temperatures show little fluctuation, it is reasonable to believe that the true temperature output of the heater based on the transformer dial setting can be found by averaging these temperatures.

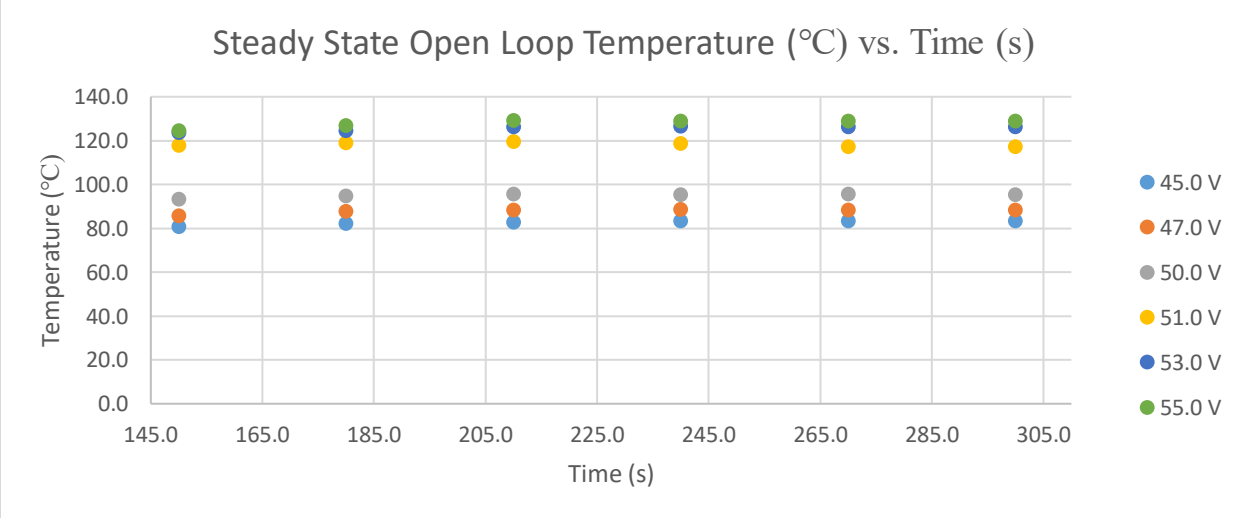

Figure 16. Steady State Open Loop Output

The graph in Figure 16 shows that the output temperatures are fluctuating very little at the point of reaching steady state. Figure 16's representation proves what the dataset in Table 4 hypothesized.

Average Temperature (°C) at Dial Reading (V)		
Dial Reading (V)	**Temperature (°C)**	**Error from Ideal**
45.0	**82.5**	**-19.5**
47.0	**87.7**	**-18.9**
50.0	**94.9**	**-18.5**
51.0	**118.2**	**2.5**
53.0	**125.5**	**5.3**
55.0	**127.7**	**3.0**

Table 5. Temperature Output (°C) at Dial Reading (V)

As stated above, it is possible to obtain the true temperature output based on the average of the found temperatures while in steady state. The dataset in Table 5 gives the average temperature in degrees Celsius based on the dial reading in voltage. The third column of the table shows the difference, or error, of the true temperature output compared to the ideal temperature output. It is worth noting that a dial setting of 50 V or below gives a large error when compared to the ideal, whereas a dial setting of 51 V or above gives a much smaller, more realistic error. It is unknown what causes such a large error; however, it can be theorized that internally the transformer's coils could be damaged in such a way that smaller voltage settings cause the inability to achieve the desired output voltages. However, without being able to take apart the transformer itself, due to lack of equipment, (only one transformer available for testing), it is not plausible to determine the exact cause.

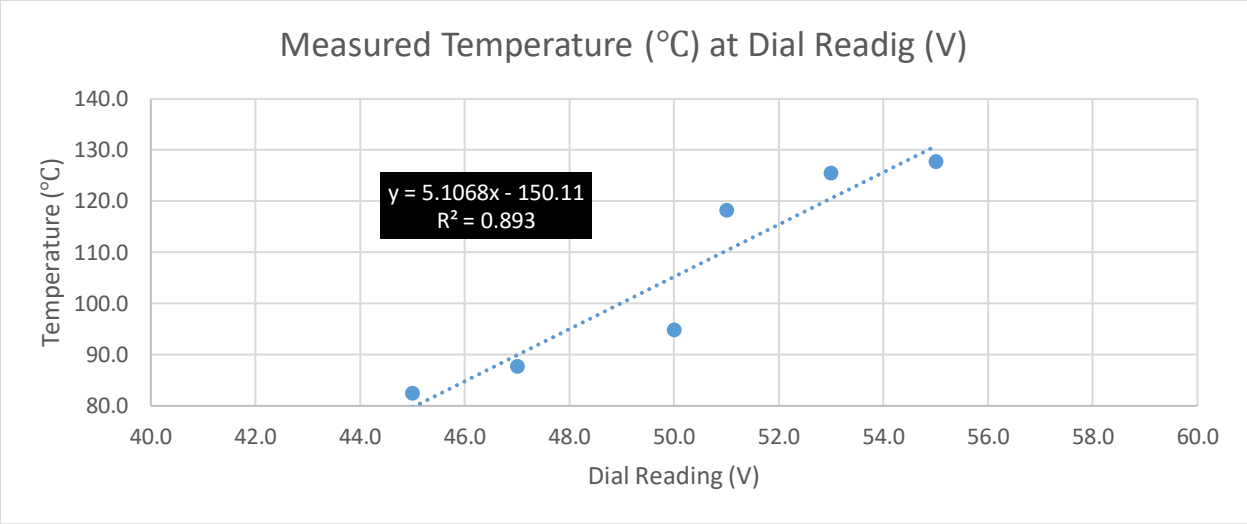

Figure 17. Measured Averaged Open Loop Output

The graphical representation of the measured temperature outputs in Figure 17 gives a visual of the temperature readings with respect to the dial voltages. The linear equation gives a modeling function to estimate the temperature based on dial reading. However, the R^2 value of .893 shows a linear function may not be the best representation for the temperature, contradicting the estimated behavior from the ideal dataset. As stated earlier, the exact cause is unknown, however because there is only one available transformer for the open loop control, the inaccuracy shows that the current setup can be improved upon.

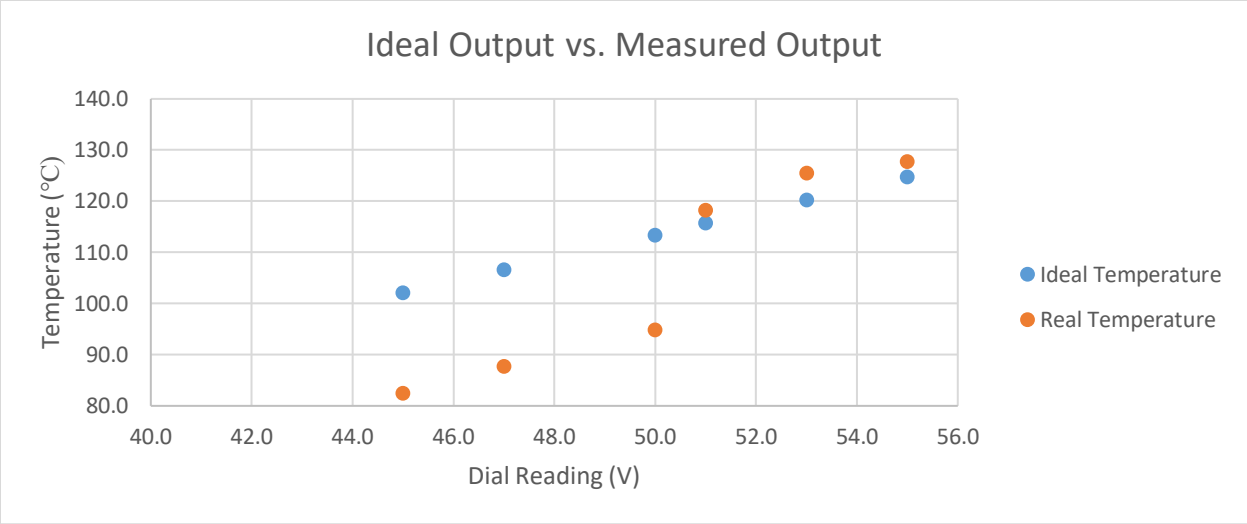

Figure 18. Measured vs. Ideal Outputs

The graph in Figure 18 is the ideal versus the measured temperature output based on the dial setting of the transformer. Figure 18 verifies what was shown in both the ideal output dataset and the real output dataset, that the real transformer output does not follow the ideal output closely. Figure 18 verifies that the accuracy of the output increases with higher dial voltages, however the graph shows that a dial reading of 2 volts lower, 54 V compared to 56 V, achieves the real desired temperature. Because the ideal dataset is based on a multiplier of 2.268, meaning the true output is off by at least 4.5 volts at the desired temperature. Inaccuracy could cause issues during testing requiring temperature control as there is a need for extra manual adjustment due to the transformer and the overall open loop control system. The non-linearity of the transformer could also cause issues for thermal testing requiring temperature other than 125 ℃, especially temperatures closer to 100 ℃ where the error is much greater.

4.2 Omega Controller

Omega Controller Temperature Feedback at Setpoint 125 ℃					
Dataset 1		Dataset 2		Averaged Dataset	
Time (s)	Temp (℃)	Time (s)	Temp (℃)	Time (s)	Temp (℃)
1.0	68.2	1.0	67.9	1.0	68.1
10.0	86.5	10.0	85.6	10.0	86.1
20.0	101.3	20.0	102.4	20.0	101.9
30.0	112.9	30.0	115.3	30.0	114.1
40.0	123.7	40.0	125.2	40.0	124.5
50.0	121.6	50.0	121.9	50.0	121.8
60.0	124.4	60.0	123.0	60.0	123.7
70.0	125.4	70.0	126.7	70.0	126.1
80.0	125.4	80.0	123.7	80.0	124.6
90.0	123.4	90.0	124.4	90.0	123.9
120.0	124.3	120.0	124.3	120.0	124.3
150.0	124.5	150.0	125.8	150.0	125.2
180.0	125.7	180.0	125.0	180.0	125.4

Table 6. Omega Controller Output (℃) vs. Time (s)

The testing for the omega controller is in Table 6. Multiple datasets were obtained and averaged in order to give the most accurate representation of what to expect based on the setpoint temperature. The testing was done over a 180 second time frame, in which the data shows the setpoint temperature was achieved in about 40 seconds, which is a much quicker rise time when compared to the required 180 seconds for the open loop system. Although there may be slightly more fluctuation of the temperature after achieving the setpoint, because of the PID architecture, the average of the oscillations gives a much closer averaged temperature output for the closed loop Omega controller compared to the open loop transformer.

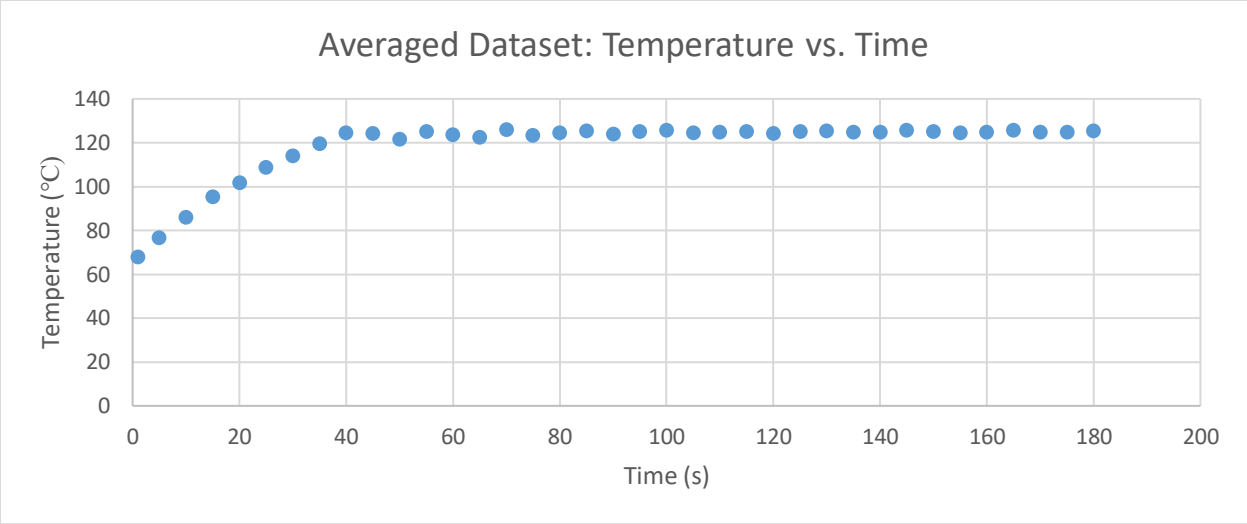

Figure 19. Averaged Omega Output

The graph in Figure 19 is based on the averaged Omega Controller Temperature output from the multiple datasets obtained. The graph verifies through visual representation that the rise time to the setpoint is roughly 40 seconds, and the fluctuations at the setpoint are minimized. These minimal fluctuations show that the closed loop system acts as a much better temperature control system when compared to the open loop control system offered by the current setup.

Omega Controller Steady State Temperature Feedback at Setpoint 125 ℃										
Dataset 1		Dataset 2		Dataset 3		Dataset 4		Averaged Dataset		Error
Time (s)	Temp (℃)	Time (s)	Temp (℃)	Time (s)	Temp (℃)	Time (s)	Temp (℃)	Time (s)	Temp (℃)	Temp (℃)
100.0	122.5	100.0	125.9	100.0	122.8	100.0	125.2	100.0	124.1	-0.9
105.0	126.6	105.0	124.2	105.0	125.2	105.0	124.6	105.0	125.1	0.1
110.0	127.3	110.0	125.2	110.0	124.6	110.0	124.7	110.0	125.5	0.5
115.0	123.5	115.0	124.4	115.0	124.1	115.0	125.6	115.0	124.4	-0.6
120.0	125.3	120.0	124.5	120.0	125.1	120.0	124.3	120.0	124.8	-0.2
125.0	127.0	125.0	125.6	125.0	124.6	125.0	124.4	125.0	125.4	0.4
130.0	123.4	130.0	125.2	130.0	124.5	130.0	125.6	130.0	124.7	-0.3
140.0	126.8	140.0	125.7	140.0	124.5	140.0	124.0	140.0	125.3	0.3
150.0	126.1	150.0	124.3	150.0	125.7	150.0	125.8	150.0	125.5	0.5
160.0	123.2	160.0	125.7	160.0	124.4	160.0	124.2	160.0	124.4	-0.6
170.0	126.7	170.0	124.2	170.0	126.2	170.0	125.6	170.0	125.7	0.7
180.0	125.1	180.0	125.4	180.0	124.1	180.0	125.0	180.0	124.9	-0.1

Table 7. Steady State Output at 125 ℃ Setpoint

Table 7 offers a closer look at the steady state output for the Omega Controller, showing after truly reaching steady state, there is very little oscillation. The four datasets were averaged out in order to give as accurate a representation for the real output as possible, and then compared to the ideal setpoint temperature. The 3 most right columns show the information previously mentioned and show that the Omega Controller operates within a ± 1 ℃ margin of the ideal 125 ℃ setpoint. Newly achieved accuracy not only is an improvement compared to the current setup, but is also based on closed loop control which takes almost all of the manual components out of the system, aside from setting the setpoint temperature.

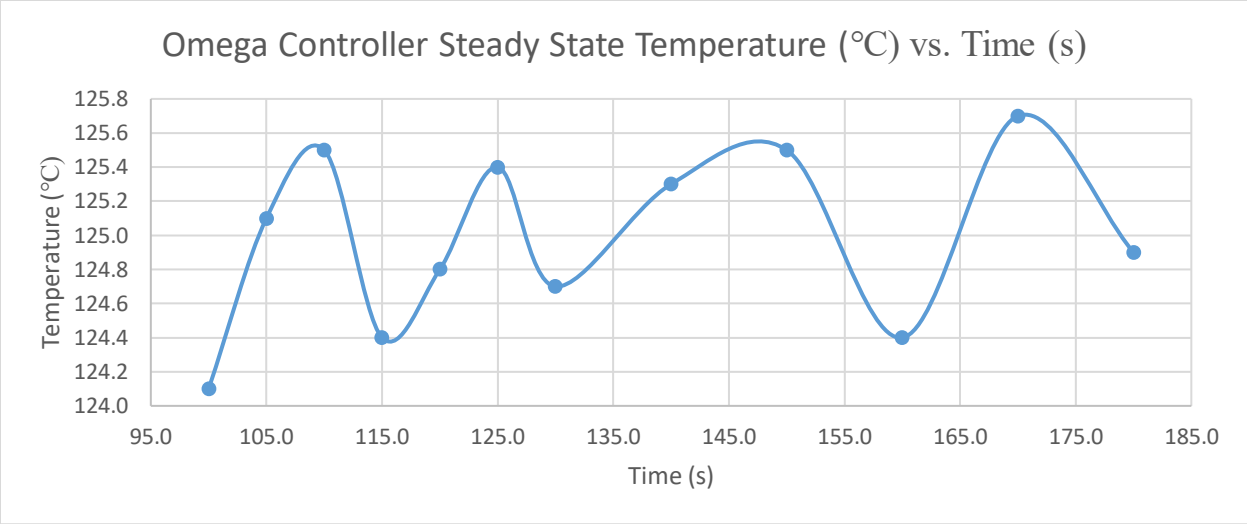

Figure 20. Steady State Omega Temperature vs. Time

The graph in Figure 20 gives the steady state temperature versus time based on the Omega Control system. The output is operating between 124 and 126 ℃ which verifies what was shown in the previous dataset. It is expected that the controller will experience some oscillations, however these oscillations will be centered around the setpoint temperature. The datapoint's mean verified accurate temperature control with the mean of the graph, which is 125.01 ℃ which is well within ± 1 ℃, even within 0.1 ℃.

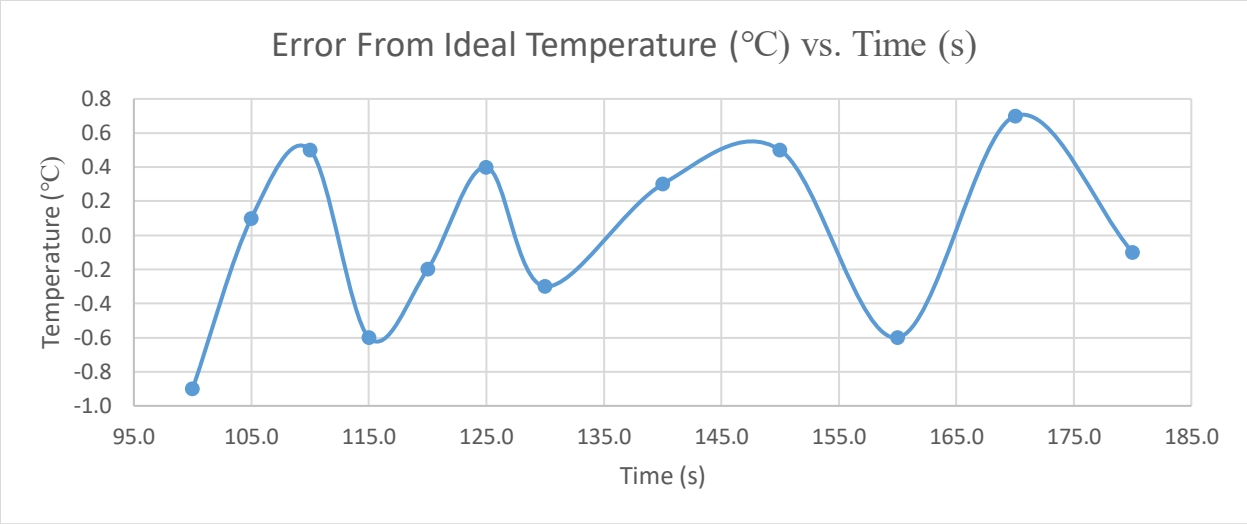

Figure 21. Error vs. Time

Figure 21 shows the error between the real temperature and the ideal setpoint temperature. Figure 21 mimics very closely the true temperature versus time graph. Because the setpoint is 125 ℃, the midpoint of the error graph is 0. Figure 21 ensures that the Omega Controller is within ± 1 ℃ and through averaging the datapoints, the average error is found to be between 0.01 and 0.02 ℃.

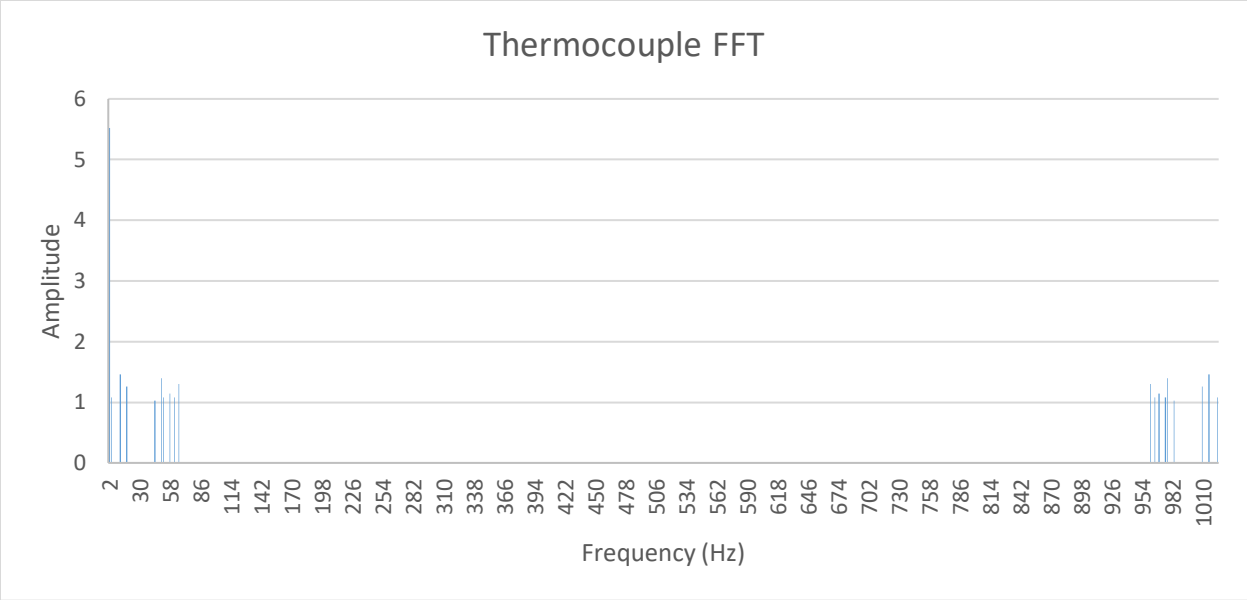

Figure 22. Fourier Transform of Thermocouple

Figure 22 shows the Fast Fourier transform (FFT) of the thermocouple which was conducted in Excel. Conducting an FFT on the temperature reading data is necessary to convert from the time domain to the frequency domain. Converting into the frequency domain provides frequencies that are present in the temperature reading data. Having more than one frequency present in the transformation shows the presence of noise on the signal. Figure 22 however, shows a large spike at a frequency of 2 Hz, with smaller spikes scattered throughout the frequency range, mostly at the extremities, close to 0 Hz and close to 1024 Hz. These spikes, however, are not worrisome when compared to the large spike at 2 Hz. A 2 Hz frequency is expected given the frequency of obtaining data occurred once every half second. Although there is some noise on the signal, the Fourier transform appears to prove the overall signal operates as it should, with little to no effect from noise.

4.3 Thermal Camera

Thermal Imaging Temperature Measurement	
Dial (V)	**Temperature (°C)**
45.0	**83.3**
47.0	**88.1**
50.0	**95.3**
51.0	**118.6**
52.0	**122.2**
53.0	**126.2**
55.0	**128.7**

Table 8. Thermal Imaging Temperature Measurement: Dial (V) vs. Temperature (°C)

The dataset in Table 8 shows the temperature in degrees Celsius with respect to the dial voltage on the transformer obtained from the thermal camera. Table 8 initially shows that the thermal camera verifies what the thermocouple showed from earlier datasets, that the true transformer output temperature is non-linear.

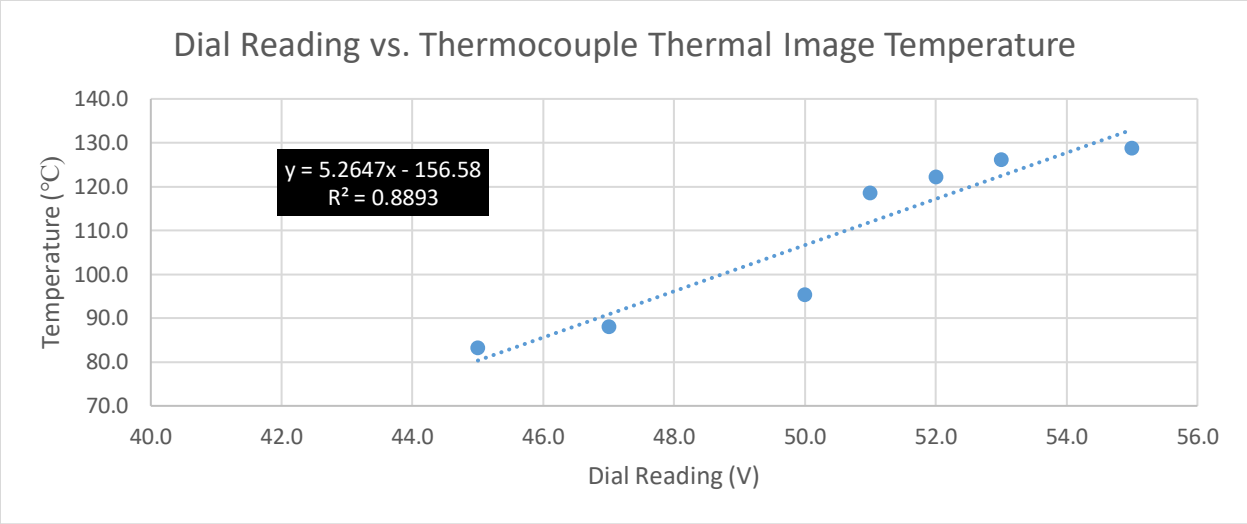

Figure 23. Dial Reading (V) vs. Thermal Image Temperature Reading (℃)

The graph in Figure 22 is a visual representation of the dataset shown in Table 8. The graph is very similar to the real temperature reading from the thermocouple. The R^2 value is close to the .893 R^2 value from the thermocouple graph. Figure 22 shows that the thermal camera, with respect to the thermocouple, reads the temperature very similarly.

Thermal Imaging vs. Thermocouple				
Thermocouple		Camera		
Dial (V)	Temperature (℃)	Dial (V)	Temperature (℃)	Difference
45.0	82.5	45.0	83.3	0.8
47.0	87.7	47.0	88.1	0.4
50.0	94.9	50.0	95.3	0.4
51.0	118.2	51.0	118.6	0.4
53.0	125.5	53.0	126.2	0.7
55.0	127.7	55.0	128.7	1.0

Table 9. Thermal Imaging vs. Thermocouple

The dataset in Table 9 shows the thermal camera reading based on different dial voltages, as well as the thermocouple reading based on different dial voltages. The last column shows the difference between the two temperature readings, showing there is at most a ± 1 ℃ difference between the two, verifying the thermal camera is as accurate as the thermocouple. For the thermal camera to calibrate the overall control system, it is necessary to perform a check, which removes the worry of inaccurate temperature readings.

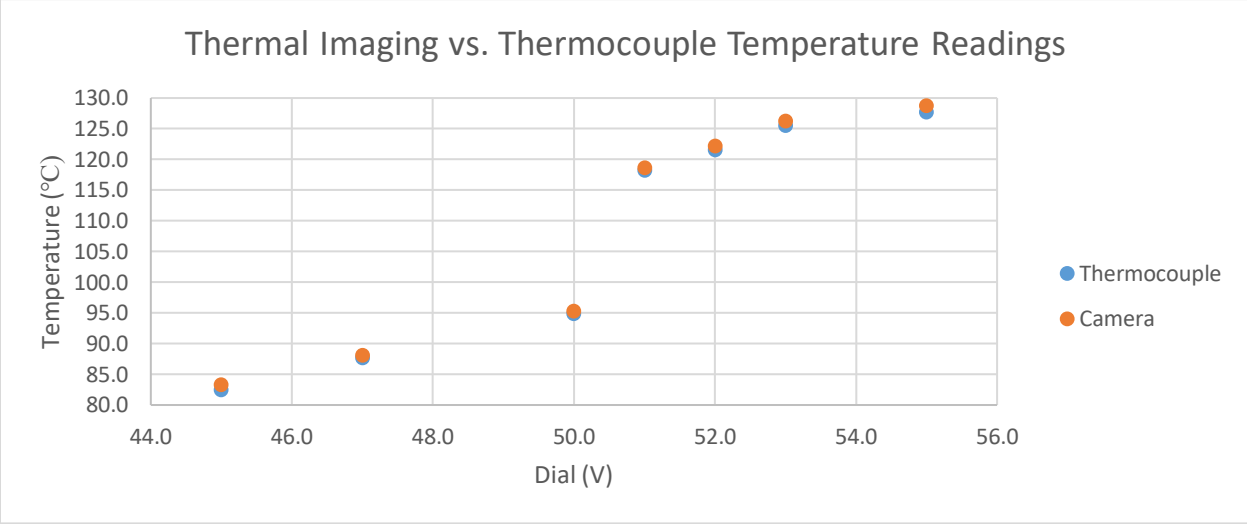

Figure 24. Thermal Imaging (℃) vs. Thermocouple (℃)

The graph in Figure 23 compares the thermal image temperature reading to the thermocouple temperature reading. Figure 23 also shows that the two are extremely close in value to each other. Figure 23's visual representation further proves the thermal camera can be used for accurate temperature readings in a similar manner to the thermocouple.

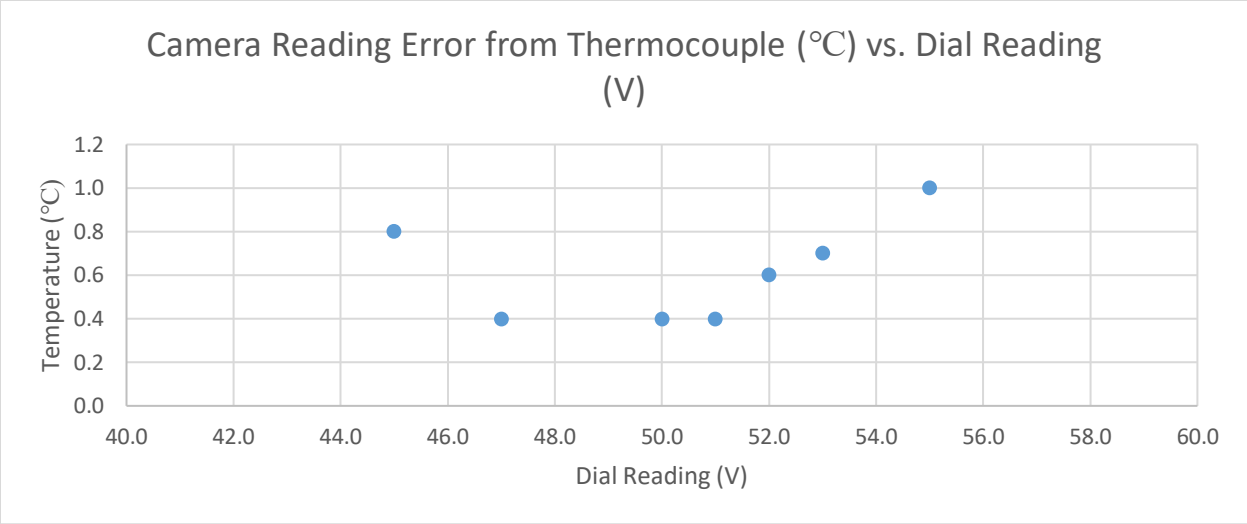

Figure 25. Thermal Image Error from Thermocouple Reading

The error graph in Figure 24 shows the most difference between the thermal camera and the thermocouple. As stated earlier, the thermal camera accuracy is at most ± 1 °C, which ensures the camera will give a similar temperature measurement compared to the thermocouple. Because of such a small amount of error, when using the thermal camera for calibration, it will be safe to assume the temperature measurement is true.

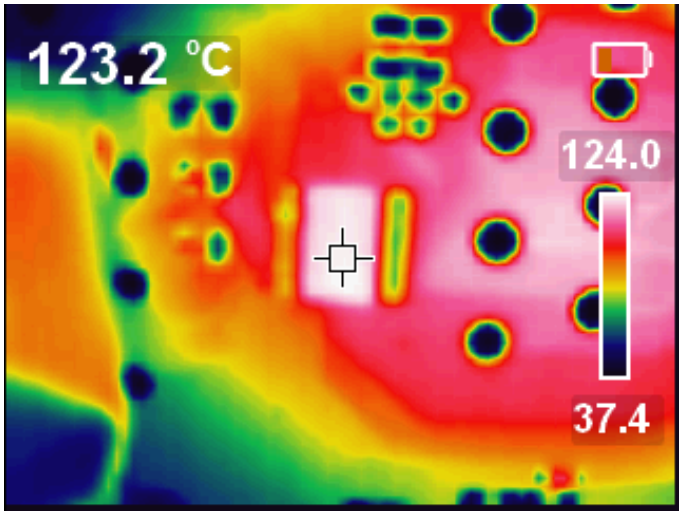

Figure 26. Thermal Image of Chip

The thermal image in Figure 25 verifies the thermal camera's ability to monitor the specific chip. If the camera could not specify the difference between the actual DUT and could only give a relative temperature of the entire PCB, then the camera could not be used to calibrate the overall control system. As seen here, the DUT's heat signature is different than the surrounding silicon, meaning the camera can accurately focus in on the DUT for calibration purposes. Thermal image also verifies the ability to monitor the DUT to ensure there is even heating and no cold spots across the entire chip. Although it should not be an issue due to the generally small package of the DUTs used for radiation testing, a larger DUT could present an issue. Having the ability to ensure even heating during radiation testing will only make the tests more accurate and could help to locate portions of the DUT that increase or decrease in heat during SEEs.

Averaged Dataset at Setpoint 125 °C					
Time (s)	Thermal Camera DUT Temperature (°C)	Error from Mean	Time (s)	Thermocouple Temperature (°C)	Error from Ideal
100.0	101.2	-0.5	100.0	124.1	-0.9
105.0	101.9	0.2	105.0	125.0	0.0
110.0	102.6	0.9	110.0	125.5	0.5
115.0	101.4	-0.3	115.0	126.0	1.0
120.0	101.5	-0.2	120.0	126.6	1.6
125.0	102.6	0.9	125.0	126.8	1.8
130.0	101.4	-0.3	130.0	126.8	1.8
135.0	101.7	0.0	135.0	126.5	1.5
140.0	101.7	0.0	140.0	126.1	1.1
145.0	101.8	0.1	145.0	125.5	0.5
150.0	102.2	0.5	150.0	125.0	0.0
180.0	100.9	-0.8	180.0	124.9	-0.1
210.0	102.1	0.4	210.0	126.2	1.2
240.0	101.7	0.0	240.0	123.8	-1.2
Mean	101.7		Mean	125.2	0.2

Table 10. Temperature (°C) vs. Time (s) at Setpoint 125 °C

The dataset in Table 10 shows the thermal camera temperature measurement of the DUT compared to the thermocouple reading which is placed at the end of the thermal force unit (TFU). By moving the thermocouple to the TFU instead of the DUT the feedback now gives the exact output temperature. Because the thermal camera handles the DUT temperature now, finding a relationship between the DUT temperature and the TFU output temperature can mathematically determine more accurate temperature control.

The setpoint of the Omega Controller was set to 125 ℃, which ensures the air coming out of the TFU would be very close to the setpoint temperature. The right-hand columns of the table show the true thermocouple temperature readings, as well as the error from the ideal setpoint. As you can see there is slight fluctuations with the temperature readings, however the average of the temperatures is very close to 125 ℃ at 125.2 ℃, well within ± 1 ℃. The left-hand columns show the thermal camera readings, which are around 102 ℃, with an average of 101.7 ℃. When comparing each of the individual temperature measurements to the average, the individual readings did not fluctuate more than ± 1 ℃. A small fluctuation verifies the DUT remains at a constant temperature after reaching steady state, as seen from the temperature measurements starting after 100 seconds. When comparing DUT temperature to the setpoint temperature, there is about a 24 ℃ difference between the TFU setpoint and the true DUT temperature when placing the TFU 1 inch, or 2.54 centimeters away from the DUT.

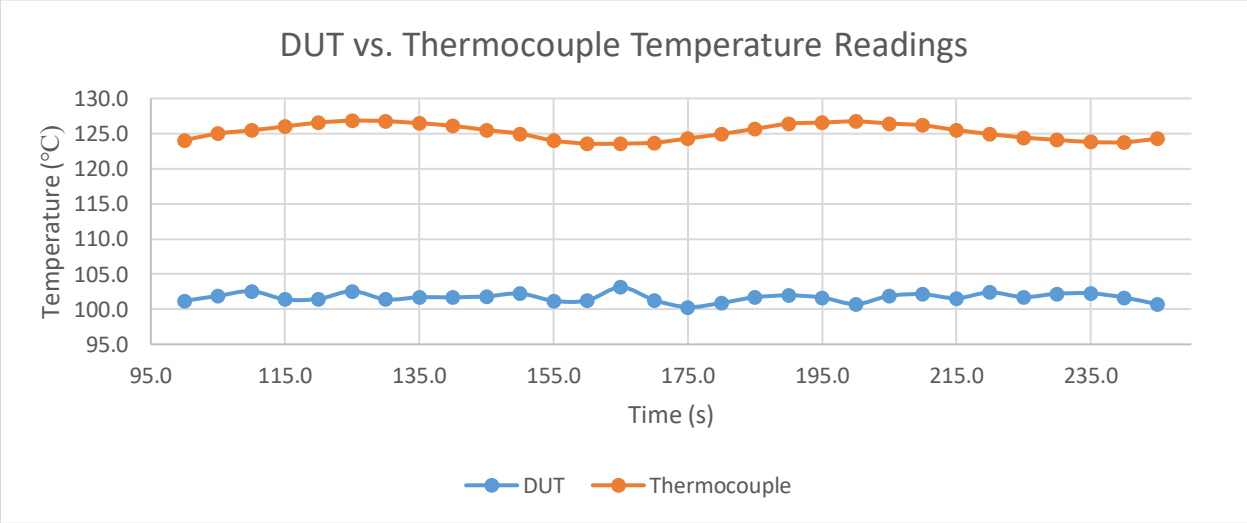

Figure 27. DUT (℃) vs. Thermocouple (℃) at Setpoint 125 ℃

The graph in Figure 26 verifies the data from Table 10. The thermocouple temperature remains centered around 125 ℃ and the DUT temperature remains centered around 101.7 ℃. The thermocouple temperature readings appear to be smoother than the DUT temperature readings, however as expected the DUT readings appear to be out of phase with respect to the thermocouple readings. Phase shifting is expected since when the thermocouple reaches its highest temperature, it will then begin to blow cooler air, which will cool the DUT down while the thermocouple still reads higher temperatures. After the controller reaches its lowest temperature, it will then blow hot air, heating the DUT while still reading lower temperatures.

Averaged Dataset at Setpoint 150 ℃					
Time (s)	Thermal Camera DUT Temperature (℃)	Error from Mean	Time (s)	Thermocouple Temperature (℃)	Error from Ideal
100.0	125.5	0.3	100.0	149.0	-1.0
105.0	125.5	0.3	105.0	150.4	0.3
110.0	125.3	0.1	110.0	150.6	0.6
115.0	124.6	-0.6	115.0	150.6	0.6
120.0	125.8	0.6	120.0	150.6	0.6
125.0	125.9	0.7	125.0	150.7	0.6
130.0	125.4	0.2	130.0	150.6	0.6
135.0	125.5	0.3	135.0	150.5	0.5
140.0	125.4	0.2	140.0	150.9	0.9
145.0	125.3	0.1	145.0	149.7	-0.3
150.0	125.2	0.0	150.0	149.6	-0.4
180.0	124.2	-1.0	180.0	150.5	0.5
210.0	125.2	0.0	210.0	150.8	0.8
240.0	126.1	0.9	240.0	149.9	-0.1
mean	125.2		mean	150.2	0.2

Table 11. Temperature (℃) vs. Time (s) at Setpoint 150 ℃

The dataset in Table 11 shows the DUT temperature based on thermal camera feedback versus the thermocouple temperature like the dataset in Table 10. Table 11, however, is based at a

setpoint of 150 ℃. The setpoint is based off the temperature differential found in Table 10 and Figure 26. Because these tables showed about a 24 ℃ difference between the TFU thermocouple and the DUT, a setpoint of 150 should give a DUT temperature of about 125 ℃. The ~24 ℃ relationship is based on the proximity of the TFU to the DUT. For testing purposes, the DUT is placed at 1 inch from the heater. Different distances could create different relationships, although with ideal placement being 1 inch, testing was performed at the ideal distance. The relationship at 1 inch apart is verified based on the DUT temperature readings, in which the mean of these temperatures is 125.2 ℃ with no more than ± 1 ℃ away from the desired temperature. The Omega controller shows a similar ability to keep the TFU output within ± 1 ℃ of the setpoint, with a mean of 150.2 ℃.

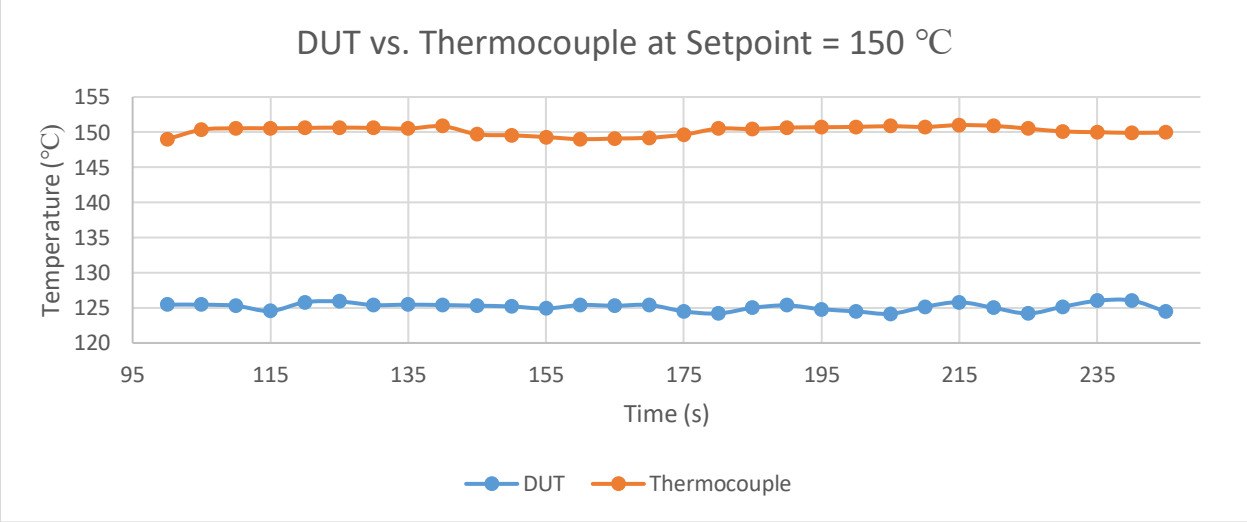

Figure 28. DUT (℃) vs. Thermocouple (℃) at Setpoint 150 ℃

The graph in Figure 27 gives a visual representation of the data from Table 11. The datapoints on the graph show that the TFU is centered around the setpoint 150 ℃ and the DUT temperature is centered around the desired temperature of 125 ℃. Like the graph in Figure 26, the

DUT is slightly out of phase with respect to the thermocouple. Figure 27 and the dataset in table 11 verify what was found in Table 10 and Figure 26 that when set 1 inch away, the DUT will be about 24 to 25 ℃ less than the TFU's thermocouple.

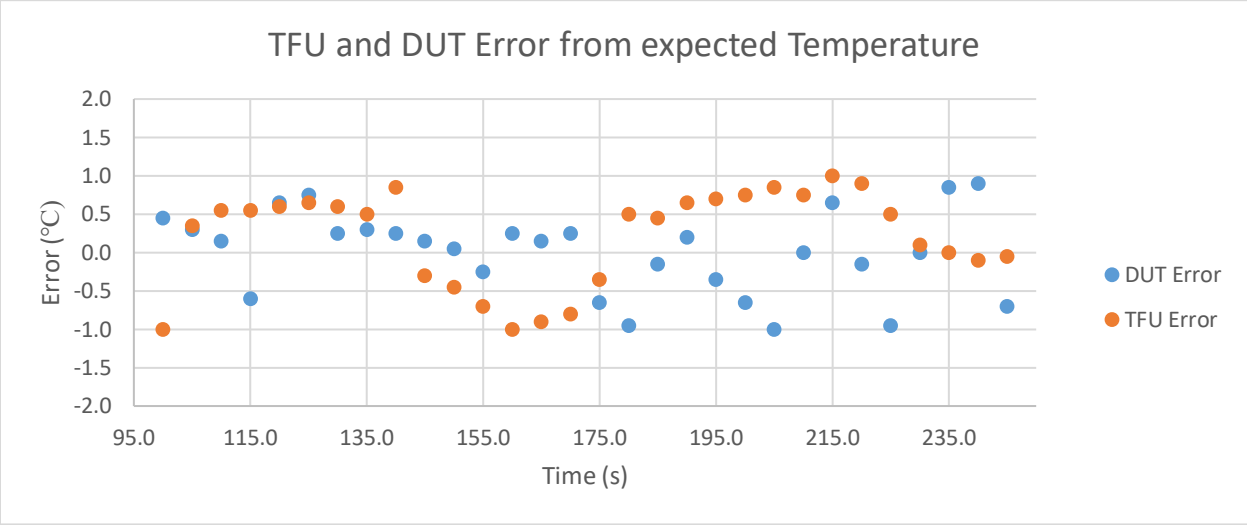

Figure 29. TFU and DUT Error from Ideal Temperature (℃)

The graph in Figure 28 shows the error from ideal temperature versus time for both the DUT and the thermocouple on the TFU. Figure 28's graph used as a visualization to show that both the DUT and the TFU do not have more than ± 1 ℃ of error. Being able to verify that the Omega Controller can keep the TFU close to the setpoint with little fluctuation, as well as verifying the DUT will not have large fluctuation further proves the obtainable accuracy.

4.4 System Comparison

The open loop control system, powered by the standalone transformer, acts as a quick, yet not very accurate solution to the issue of temperature control. This issue rises from the lack of resolution of the transformer itself. Although open loop control can be as accurate as closed loop control, this specific system is hindered by the transformer only adjusting by 1 volt at a time. A smaller resolution, such as .1 volt at a time would increase the overall accuracy of the open loop system. The open loop control system is portable, containing of only the standalone transformer, the TFU, the air pressure gauge, and any connecting tubes for pressurized air. The open loop control system is easy to transport and can be used at any location if there are enough outlets or extension cords for setup. It also offers the ability for thermocouples to be taped close to the DUT for feedback into a LabVIEW GUI for numerical or graphical feedback. However, the system is still open loop, and has no way of correcting itself without the need for manual implementation. Along with needing manual implementation, because the manual implementation involves rotating the voltage dial, the actual output voltage for a desired voltage can be different depending on who is operating it. Once the dial is set, the open loop system requires a long rise time to achieve its final output temperature, needing at least 120 seconds to reach steady state. Although two minutes may not seem like much time in the long run, when conducting radiation testing, every second counts. The less time needed to adjust the system and wait for it to reach its desired temperature, the more testing can be done.

In contrast, the Omega Controller is a closed loop automated control system. Much like the open loop control system it is portable and can be setup and virtually any location. Unlike the open loop system, the Omega Controller needs only about 35 to 40 seconds to reach its setpoint and settles to the setpoint with no more than ± 1 ℃ of fluctuation. Because of the small fluctuation, the average output of the TFU is very close to the setpoint, with a per run average of ± .2 ℃ off

from the setpoint, and an overall average of ± .01 ℃. An ability to control the temperature to such a high degree offers the accurate control that the open loop control system cannot offer. Like the open loop control system, the thermocouple offers feedback into a LabVIEW GUI for numerical and graphical feedback to ensure the control system is acting as expected. However, the Omega Controller system is still dependent on feedback from a thermocouple, like the open loop control system. If the thermocouple is not placed at the end of the TFU, then the thermal couple, like the open loop control system, must be placed as close to the DUT as possible. Relying on proximity could cause issues between what the thermocouple is reading versus what the DUT temperature is. Because of a proximity issue, there is a need to improve on the Omega Controller so that temperature adjustments can be based on the actual DUT temperature not just a thermocouple at the TFU or a thermocouple taped somewhere close to the DUT on the PCB.

As a partial solution to the issue stated in the above paragraph, implementing a thermal camera as part of the Omega Control system to create an overall thermal camera control system helps to solve the issue of DUT temperature versus thermocouple temperature. The thermal camera offers a non-contact temperature measurement method, which means no longer is the "DUT temperature" measured via thermocouple, it is now measured using infrared imaging technology. Non-contact methods mean that the camera can be placed out of the way of the beam if there is a clear view to the DUT and can measure the true DUT temperature. These temperature readings can be saved as images to an SD card on the camera that can easily be uploaded to a laptop or PC through USB. Unlike the numerical or graphical feedback achieved from the thermocouple, the images can show what is happening at the DUT, as seen in Figure 25. The operator can be sure that not only is the DUT temperature being received, but also that the setup of the TFU is correct so that the DUT is being heated evenly. However, because the current thermal camera requires

someone to manually take a picture, the system is not completely automated. In order to transfer data to a LabVIEW GUI, images would first have to be uploaded to the PC and then put into the GUI via user input. Although a new thermal camera control system does not offer complete automated control, there is an ability to use the set of images obtained from the thermal camera as a one-time calibration in order to adjust the setpoint of the Omega Controller so that the DUT temperature reaches the desired temperature.

Although each system has its own pros and cons, the Omega control system offers control that the current open loop control system, with the resolution of the transformer, cannot achieve. However, because the Omega control system still relies on thermocouple feedback, it is not perfect. Because of the Omega Controller's imperfections, implementing the thermal camera with the Omega control system creates a system that does not directly rely on thermocouple feedback for DUT measurements. The thermal camera control system still needs some improvement in order to operate optimally, however, the thermal camera control system is a vast improvement on the current open loop control system and offers portable accurate temperature control previously only achieved in stationary climatic chambers.

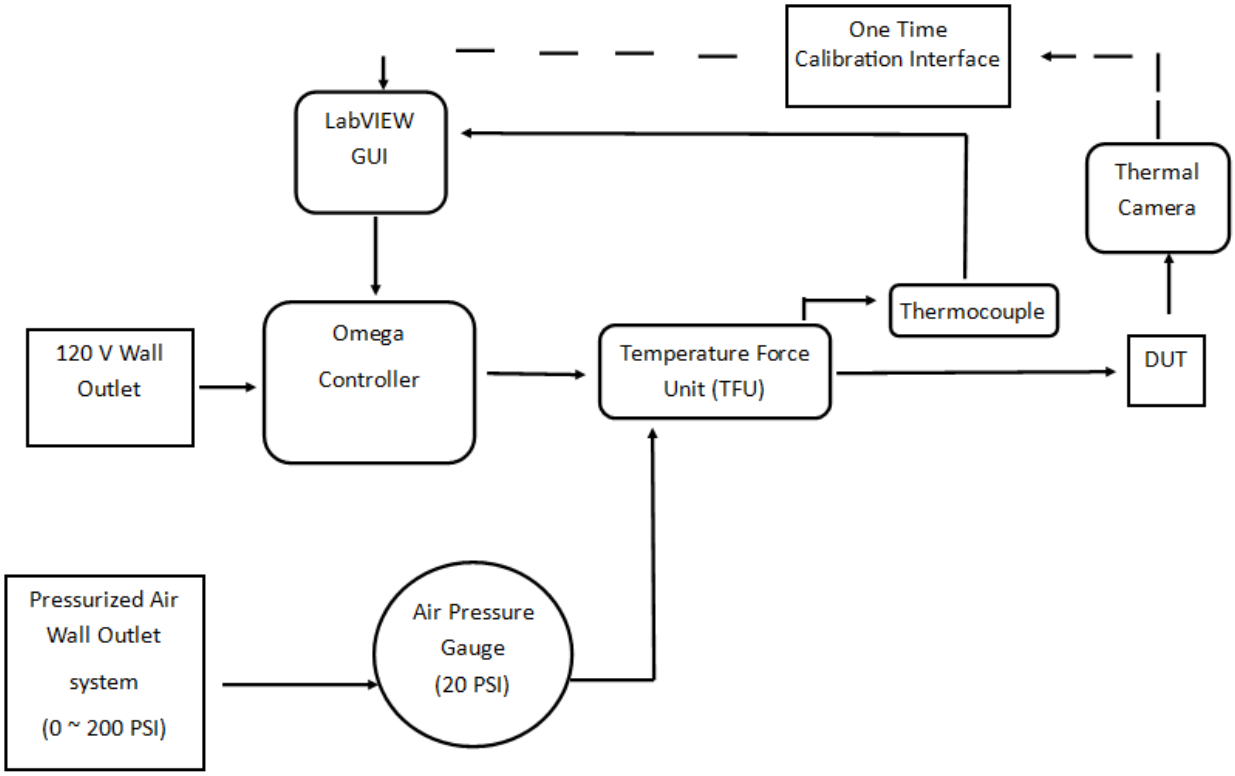

Figure 30. Proposed Complete System Block Diagram

The block diagram in Figure 29 is a representation of how the overall thermal camera control system will work. The pressurized air will come from an outlet hose which is fed into an air pressure gauge set to about 20 PSI, which will then be fed to the TFU which acts as a forced air flow heater. The TFU will receive a voltage from the Omega Controller, which is plugged into a 120 V outlet to receive its power. The amount of voltage forced to the TFU is decided based on the setpoint on the LabVIEW GUI as well as the feedback from the thermocouple which is placed at the end of the TFU. The thermal camera will then take a set of images of the DUT in order to achieve an accurate temperature measurement and ensure the DUT is being heated evenly. The operator of the thermal camera will then make a one-time calibration to the setpoint on the LabVIEW GUI to ensure the output temperature of the TFU is at the correct temperature to achieve the desired DUT temperature.

5. CONCLUSION AND FUTURE WORK

5.1 Conclusion

Conducting thermal tests on devices for a terrestrial environment is an important proponent of most characterization testing. When conducting these thermal tests, no worries surround climatic chambers “blocking” anything, therefore the chamber method is viable and widely used. However, when conducting radiation testing, there is a need for a specific DUT(s) to be bombarded with heavy ion radiation in order to mimic the LET and dosage the part would see in its orbit. A normal climatic chamber will only work if conducting in house testing, and with most companies not having the ability to do so, a portable system with accuracy like a climatic chamber is necessary. Based on the research conducted, the Omega Controller can offer similar PID control for TFU temperature much like a climatic chamber. Like a climatic chamber, the PID loop will be able to overcome environmental effects that an open loop control system would not be able to account for. Along with this, the resolution of the Omega Controller is a vast improvement on the resolution of the open loop’s transformer. Running the Omega Controller with a GUI offers quick and easy setup and configuration for both pretest setup and in test adjustments. Utilizing thermal imaging technology provides accurate DUT measurements, given the entire PCB will not be heated like a climatic chamber would do. The thermal image will also ensure even heating of the DUT, which will verify both the accuracy of the TFU and the accuracy of the tests.

5.2 Future Work

Although the system is a vast improvement on the current setup, as well as acts as a portable and accurate semi-automated control system, the system is not perfect. Future work that could be done would include testing in the cyclotron environment at Texas A&M University, however with the cyclotron shut down in the early months of the Spring semester, the timetable did not align in order to conduct temperature control tests there. These tests would obtain more true results, given a cyclotron is the environment the system will be working in. With the current thermal camera, there is an inability to transmit temperature measurement directly to a computer without manual input, and no way to adjust the TFU temperature without manually typing the new setpoint into the LabVIEW GUI. A possibility to solving camera issues would be procuring a higher end thermal camera than can connect directly to the Omega Controller. A better camera would eliminate the one-time calibration element, as well as eliminate the need for two different temperature measurements. The thermal camera would feed the DUT temperature directly into the Omega Controller, which would then adjust the output temperature solely on the DUT temperature. A second possibility for future work with respect to the camera would be to procure a camera which could connect to a Raspberry Pi or Arduino in order to create an IOT based measurement system, in which the Pi or Arduino would transmit measurements via Wi-Fi or Bluetooth to the LabVIEW GUI. If either of these types of cameras could be procured to eliminate the one-time calibration component of the system to make the temperature control portion of the system automatic, a control system for the camera could be implemented in order to remove the need for manual setup of the camera. If the locations of the DUTs on their respective PCBs were known, then implementing a control system that could adjust the camera automatically based on the board

would eliminate all manual components aside from setup and take down. If camera procurement is not an option, the current thermal camera control system could be improved upon by using modeling and simulation. By modeling the DUT temperature relative to the TFU temperature, the accuracy of the system could be improved by determining the relationship between the two in greater detail. Through simulations, one could also determine how the DUT temperature and TFU temperature will react at different distances. Although 1 inch is the ideal positioning from the DUT, simulation could show different distances, which could be useful in the event TFU positioning is required to be further away than preferred. Along with distance simulations, different angles of TFU setup could be explored in order to see if, and how much, the angle of the TFU affects the DUT temperature.

REFERENCES

[1] Rebollo, Francisco Javier Aparicio. “Thermal Cycling on Electronic Components” *EEE Parts,* wpo-altertechnology.com/thermal-cycling/. 2019. Accessed 16 Mar. 2020.

[2] OMEGA. “What is a PID Controller” omega.com/en-us/resources/pid-controllers. 17 Apr. 2019. Accessed 16 Mar. 2020.

[3] Baumann, Robert et al., “Radiation Handbook for Electronics” TI.com/radbook. 2019. Accessed 16 Mar. 2020.

[4] Gawalt, Brian. “Gawalt redesign.jpg” vis.berkely.edu/courses/cs294-10-fa07/wiki/index.php/image:Gawalt_redesign.jpg. 12 Sep. 2007. Accessed 16 Mar 2020.

[5] Barth, Janet L. “Space and Atmospheric Environments: from Low Earth Orbits to Deep Space” *NASA/Goddard Space Flight Center.* Ntrs.nasa.gov/archive/nasa/casi.ntrs.nasa.go/2000053331.pdf. 2003. Accessed 16 Mar. 2020

[6] Texas A&M University Cyclotron Institute. “Radiation Effects Facility” cyclotron.tamu.edu/ref. 2019. Accessed 16 Mar. 2020.

[7] Badhwar, Gautam D. “The Radiation Environment in Low-Earth Orbit.” *Radiation Research*, vol. 148, no. 5, 1997, pp. S3–S10. *JSTOR*, www.jstor.org/stable/3579710. Accessed 15 Mar. 2020.

[8] Ghaffarian, Reza, “Accelerated Thermal Cycling and Failure Mechanisms for BGA and CSP Assemblies” nepp.nasa.gov/docuploads/99810235-C28A-4A8D-BD52223A33EF7CDF/ASME-Hawaii993-lockeed.pdf. 2000. Accessed 16 Mar. 2020.

[9] University of Maryland, “Thermal Shock” *Center for Advanced Life Cycle Engineering.* Calce.umd.edu/thermal-shock. 2020. Accessed 16 Mar. 2020

[10] Flicker, Jack David, Tamizhmani, Govindasamy, Moorthy, Mathan Kumar, Thiagarajan, Ramanathan, and Ayyanar, Raja. Accelerated testing of module-level power electronics for long-term reliability. United States: N. p., 2016. Web. doi:10.1109/JPHOTOV.2016.2621339.

[11] Battalwar, Pooja et al. “Infrared Thermography and IR Camera.” https://www.semanticscholar.org/paper/Infrared-Thermography-and-IR-Camera-Battalwar-Gokhale/2a24b0240376c3c5a1dfd213284ff8fdaf647674. 2015. Accessed 16 Mar. 2020.

[12] T. J. Bajzek, "Thermocouples: a sensor for measuring temperature," in IEEE Instrumentation & Measurement Magazine, vol. 8, no. 1, pp. 35-40, March 2005.

[13] J. Liu, L. Ma and J. Yang, "Methods and techniques of temperature measurement," 2011 International Conference on Electrical and Control Engineering, Yichang, 2011, pp. 5332-5334.

[14] M. M. M. Flores et al., "Implementation of Control Algorithms in a Climatic Chamber," 2016 International Conference on Mechatronics, Electronics and Automotive Engineering (ICMEAE), Cuernavaca, 2016, pp. 107-112.

[15] Astrom, Karl Johan, “PID Control” *Control System Design*. Cds.caltech.edu/~murray/courses/cds101/fa02/Caltech/astrom-ch6.pdf. 2002. Accessed 16 Mar. 2020.

[16] Bennett, Stuart, “The Past of PID Controllers” *Department of Automatic Control & Systems Engineering.* www.researchgate.net/publication/317148536. Apr. 2000. Accessed 16 Mar. 2020

[17] National Instruments, “PID Control Using LabVIEW” ni.com/tutorial/6440/en/#toc2. 11 Feb. 2020. Accessed 16 Mar. 2020.

[18] Payne, Lee, “The Modern Industrial Workhorse: PID Controllers” *Motion Control*. Techbriefs.com/component/content/article/tb/features/articles/20013. 1 Jul. 2014. Accessed 16 Mar. 2020

[19] Farnell, “116C-216C and 117C-217C Series” Farnell.com/datasheets/1519735.pdf?_ga=2.119084169.1437196335.1580498119-945573144.1580498119. Accessed 16 Mar. 2020.

[20] Omega, “User’s Guide” *CSi8DH Series Benchtop Controllers.* Newportus.com/Pdf/M3906.pdf. Accessed 16 Mar. 2020.

[21] Huepar, “Pocket-Sized IR Thermal Imager, Temperature Tracking & Adjustable Emissivity HTI80P” *Products.* https://www.huepar.com/products/pocket-sized-ir-thermal-imager-huepar-80-x-60-infrared-resolution-thermal-imaging-camera-measurement-range-14-f-752-f-with-76800-pixels-display-temperature-tracking-adjustable-emissivity-hti80p. 2020. Accessed 16 Mar. 2020.